Atmos. Chem. Phys., 25, 10965–10986, 2025
https://doi.org/10.5194/acp-25-10965-2025

Atmospheric Chemistry and Physics
Open Access
EGU

New water-soluble, toxic tracers of wood burning identified in fine brown carbon aerosol using a non-target approach

Vinh Nguyen, Bartłomiej Witkowski, and Tomasz Gierczak

Faculty of Chemistry, University of Warsaw, al. Żwirki i Wigury 101, 02-089 Warsaw, Poland

Correspondence: Bartłomiej Witkowski (bwitk@chem.uw.edu.pl)

Received: 17 March 2025 – Discussion started: 31 March 2025
Revised: 22 July 2025 – Accepted: 6 August 2025 – Published: 23 September 2025

Abstract. The molecular composition of water-soluble fine (PM_3) brown carbon aerosol (BrC_{aq}) generated by the combustion of wood was studied with ultra-performance liquid chromatography coupled with electrospray ionization time-of-flight mass spectrometry (UPLC-ESI-ToF/MS) using a non-target analysis (NTA) workflow. The NTA analysis workflow based on MS-DIAL and MS-FINDER showed the best performance of the five software tested. Structures of 361 out of the 420 water-soluble organics in BrC were tentatively identified for the first time. The total emission of fine, water-soluble BrC_{aq} was approx. 1 g kg^{-1} of wood burned, comparable with the emission factors of some semi-volatile organics from open biomass burning. Potential precursors of aqueous secondary organic aerosols ($_{aq}$SOAs) and toxic molecules were selected among the newly identified molecules.

The newly identified harmful tracers of fine BrC included plant and wood care products, alkaloids, and fungal metabolites. Fungal metabolites were also identified among the potential precursors of $_{aq}$SOAs with high Henry's law constant values, alongside natural compounds occurring in roots and leaves, diterpenoids, flavonoids, anthraquinones, and coumarins. The release of these natural and man-made compounds is possible during wildfires and domestic uses of biomass. The atmospheric lifetimes calculated for the newly identified precursors of $_{aq}$SOAs showed that natural dyes, bacterial and fungal metabolites, and (aromatic) glucosides can undergo aqueous OH oxidation in cloud water. Such molecules can produce low-volatility products without decomposing due to their large carbon backbones. Many new potential chromophores were also identified in BrC, including natural dyes and molecules with conjugated double bonds and aromatic rings.

1 Introduction

Biomass is organic material from plants and animals and often refers to non-fossil fuels, like wood, pellets, and straw. Biomass is used around the globe for generating heat and energy, including domestic and industrial uses (Antar et al., 2021; Tomlin, 2021). Over 3 billion people use solid (bio)fuels for cooking and heating, which globally accounts for 41 % of households (Amegah and Jaakkola, 2016). Open biomass burning (BB) is also widespread in some regions due to cultural and economic practices (Admasie et al., 2018). Furthermore, the use of biomass aims to limit the reliance of the energy sector on nonrenewable fossil fuels and to decrease the net emissions of greenhouse gases (GHG) (Tomlin, 2021). At the same time, the large-scale use of biomass as a renewable, carbon-neutral fuel in power and heating plants remains debatable (Stubenrauch and Garske, 2023).

Open BB includes burning crop residues (Hartner et al., 2024), vegetation fires intensified by man-made climate change (Jones et al., 2024). Around the globe, more frequent and widespread wildfires pose a serious threat to humans, infrastructure, and ecosystems. In the 2023–2024 fire season, the global area burned is estimated at 3.9×10^6 km^2, causing many fatalities and billions of dollars in damages in the US, Canada, the EU, and Asia (Jones et al., 2024).

In addition to direct exposure effects, open BB emits large amounts of pollutants, which can affect areas far from the source (Jones et al., 2024; Laskin et al., 2025). BB is a ma-

jor global source of methane (5 %–15 %), CO (30 %–50 %), NO_x (20 %), anthropogenic CO_2 (18 %), and the second-largest source of non-methane volatile organic compounds (VOCs) (Pan et al., 2020). Furthermore, BB is the major source of black carbon (BC) and primary organic aerosols, accounting for 57 ± 2 % and 87 ± 2 % of the global emissions, respectively (Andreae, 2019; Jiang et al., 2024). BC and organic aerosols, including also light absorbing aerosols, the so-called brown carbon (BrC) emitted by BB, account for up to 70 % of the total emission of fine particulate matter ($PM_{2.5}$) into the atmosphere (Jiang et al., 2024; Yadav and Devi, 2019).

BB pollutants, including GHGs and fine PM, affect the air quality and climate and harm human health (Jiang et al., 2024). All fine PMs influence the hydrological cycle by initiating the formation of clouds and ice crystals (Bellouin et al., 2020). Fine aerosols, including biogenic secondary organic aerosols (BSOAs) (Tsigaridis and Kanakidou, 2018), also scatter light, thereby reducing the amount of radiation reaching the Earth's surface (Kahn et al., 2023). Unlike most BSOAs, BC and BrC absorb the incoming solar radiation, exhibiting positive radiative forcing, which increases global temperature (Laskin et al., 2025).

Due to its high atmospheric abundance, BC is the second largest contributor to man-made radiative forcing (Matsui et al., 2018). The contribution of BrC to the direct radiative forcing of BC is likely substantial, but the estimates vary between 20 % and 70 % (Laskin et al., 2025). BC absorbs light from infrared (IR) down to the ultraviolet (UV) region, whereas BrC exhibits a much narrower (wavelength-dependent) absorption in the UV-Vis region of the electromagnetic spectrum (Saleh, 2020; Laskin et al., 2025).

The radiative forcing of BrC estimated by global models varies from 0.03 to 0.57 $W\,m^{-2}$ (Li et al., 2023). This uncertainty is, in part, due to incomplete data about the sources, formation mechanisms, atmospheric transformations, light absorbance, and chemical composition of BrC (Li et al., 2023). For this reason, identifying the pollutants emitted from combustion sources has been the subject of extensive research (Li et al., 2023; Young et al., 2021). Thousands of unique molecules contribute to BrC aerosols, including saccharides, halogenated, nitrated, and halogenated phenols, polycyclic aromatic hydrocarbons, terpenoids, resin acids, dioxins, alkanes, oxygenated and aromatic, and organosulfur compounds etc. (Divisekara et al., 2023; Young et al., 2021; Brege et al., 2021). At the same time, most of these compounds remain unidentified because a comprehensive, molecular-level characterization of BrC presents a considerable analytical challenge (Brege et al., 2021; Divisekara et al., 2023; Laskin et al., 2025).

Furthermore, the chemical composition of BrC is not only forbiddingly complex but also evolves during transport and chemical processing (the so-called chemical aging) in the atmosphere (Moise et al., 2015; Laskin et al., 2025). Formation and evolution of BrC in the atmosphere involve various gas, aqueous, and multiphase reactions, such as chemical aging by UV radiation and inorganic radicals (Zhao et al., 2015). Particularly, the currently poorly characterized (photo)chemical processing of BB emissions in atmospheric hydrometeors largely influences the composition, light absorption, and toxicological and physicochemical properties of BrC (Wong et al., 2019; Choudhary et al., 2023). For instance, the aqueous oxidation of BrC by OH initially enhanced the UV-Vis absorbance but led to bleaching following prolonged exposure (Lei et al., 2025; Hems et al., 2020). However, due to the limited data on the water-soluble organic compounds (WSOCs) emitted by BB, our understanding of the climate and health effects of BrC remains incomplete (Li et al., 2023).

This work aimed to study the WSOCs in fine BrC (BrC_{aq}) emitted by the pyrolysis of woody biomass, focusing on toxic molecules and those with high Henry's law constant (H, $M\,atm^{-1}$) values. The latter group can dissolve in atmospheric hydrometeors and undergo further chemical processing, resulting in (light-absorbing) aqueous secondary organic aerosols ($_{aq}$SOAs) (Lei et al., 2025; Go et al., 2024). $_{aq}$SOAs are likely important but still poorly characterized compounds of fine atmospheric PM (Su et al., 2020).

In the work presented, to gain detailed, molecular-level insights into the composition of BrC_{aq}, analyses were carried out with ultra-performance liquid chromatography coupled with electrospray ionization time-of-flight mass spectrometry (UPLC-ESI-ToF/MS) using a non-target analysis (NTA) workflow. NTA identifies (annotates) unknown compounds based on the high-resolution mass spectrometry (HR-MS) data using databases and *in-silico* fragmentation prediction (Hulleman et al., 2023; Vosough et al., 2024). Therefore, NTA is a promising approach for resolving the molecular complexity of BrC (Laskin et al., 2025). This work presents the first application of NTA in analyzing BrC_{aq} generated by wood pyrolysis (Divisekara et al., 2023; Young et al., 2021; Hartner et al., 2024).

The immense amounts of data generated by the modern LC/MS and GC/MS instruments require advanced processing algorithms, involving deconvolution, feature detection, and annotation (Hohrenk et al., 2020). Over the past decade, there has been a considerable increase in the availability of software for HR-MS data mining (Hohrenk et al., 2020). However, the number of features extracted and identified in NTA largely depends on the data processing workflow (Hohrenk et al., 2020; Wartmann et al., 2024). For this reason, several NTA workflows were tested in this work, including competitive Fragmentation Modeling for Metabolite Identification (CFM-ID) (Wang et al., 2021), Metaboanalyst (Pang et al., 2024), Global Natural Products Social Molecular Networking (GNPS) (Aron et al., 2020), MS-DIAL, MS-FINDER (Tsugawa et al., 2015), and MZmine (Schmid et al., 2023), using a mixture of model BB pollutants. Afterward, the best-performing workflow was used to analyze BrC_{aq}.

Here, BrC was generated in the N_2 atmosphere in a new, custom-designed combustor. Wood pyrolysis was conducted to simulate combustion conditions during vegetation fires, as oxygen is absent inside logs and in the deeper zones of the fire (Chen and Bond, 2010; Sekimoto et al., 2018; Divisekara et al., 2023; Gao et al., 2024). The composition of BrC_{aq} was compared with the previously published data, and > 360 tracers of wood pyrolysis were tentatively identified for the first time. Several WSOCs in BrC_{aq} with high H values and toxicities (LD_{50}) were also first identified in this work.

Additionally, quantitative analysis was performed with LC/MS using surrogate standards to identify the major components of BrC_{aq} (Pieke et al., 2017). Quantitative results obtained using surrogate standards, a total organic carbon (TOC) analyzer, and the gravimetric method showed that estimating relative ionization efficiencies for WSOCs in BrC_{aq} yielded reasonably accurate results.

2 Experimental section

Materials and reagents are listed in Sect. S1 in the Supplement.

2.1 Biomass combustor and fine particle collection

A diagram of the newly constructed biomass combustor is shown in Fig. 1.

The combustor consisted of a 3 kW cylindrical resistance heater with a round steel base that was placed on top of a heat-insulating board – Fig. 1. The heater was secured to the base with heatproof cement, and surrounded by a 5 cm thick layer of fireproof insulation. The outer wall of the combustor was a steel cylinder with an additional layer of a heat-reflecting mat. The combustor base was equipped with the bath gas inlet, which ran inside the insulating board – Fig. 1. A controller was used to adjust the combustion temperature within ±5 °C. Pellets were placed in a ceramic crucible with a K-type thermocouple connected to the temperature controller and inserted in the middle of the fuel stack. The flow of batch gas and the pumping speed were adjusted with manual valves, and the pressure inside the combustor was 1 atm.

Mixed wood pellets (25 g) were heated at 350 °C for 2 h, and the bath gas flow (N_2) was maintained at 1.5 L min^{-1}. The stream from the combustor cooled down to approx. 80 °C before reaching the sampling assembly. First, the emissions passed through a stainless steel mesh filter (mesh size 0.5 mm–50 µm, Fig. 1) to remove coarse particles. Afterward, two 47 mm filters were used; the first filter (hydrophobic PTFE, pore size 3 µm, Fluoropore, FSLW07400) was followed by a second PTFE-coated glass microfiber filter (EMFAB TX40H120-WW, Pallflex, aerosol retention 99.95 %). During sampling, both filter assemblies were kept at 80 °C using a heating sleeve (10 cm I.D., not included in Fig. 1) to avoid condensation of water and other semi-volatiles.

Before sampling, filters were placed in a desiccator with dry molecular sieves for 24 h. Particles collected on the second filter (PM_3) were extracted using 2 mL of water via mechanical agitation and filtered through a 0.22 µm PTFE filter before analysis. The extracts were diluted tenfold before LC/MS analysis to prevent ion source contamination and minimize matrix effects on the semi-quantitative results (see Sect. 2.5).

2.2 Liquid chromatography coupled to mass spectrometry

Analyses were performed using the Q-TOF LCMS-9030 system (Shimadzu) using an Acquity HSS-T3 column (Waters, 100 mm × 2.1 mm, 1.8 µm). The mobile phase consisted of 0.1 % formic acid in water (eluent A) and 0.1 % formic acid in ACN (eluent B); the injection volume was 2 µL. The mobile phase flow rate was 0.25 mL min^{-1}, and the column temperature was 30 °C. The gradient elution program involved adjusting the amount of eluent B as follows: initially, 5 % for 10 min, then linear increase to 25 % over 5–22 min; held at 25 % for 13 min, then linear increase to 95 % over 35–39 min, held at 95 % for 5 min, then linear decrease to 5 % over 1 min, and held at 5 % for 5 min. The total analysis time was 50 min.

The mass spectrometer was equipped with an electrospray ion (ESI) source, operating in positive or negative ionization modes. The nebulizing, drying, and heating gas flows were set at 3.0, 10, and 10 L min^{-1}, respectively. The interface temperature was 300 °C. The TOF mass resolving power was approx. 45 000. Spectra were collected in the data-dependent acquisition (DDA) mode; m/z 100–600 (precursor selection, even time 1 s), m/z 40–600 (product ion scan, even time 0.1 s), number of dependent events 3, intensity threshold 3000, delay time 1 s, charge state 1. Each sample was analyzed six times, at positive and negative ionization modes utilizing three collision energy (CE, V) values: 0–7 V for (low), 10 ± 5 V (medium), and 17 ± 5 V (high), and the CE spread was 5 V. After adjusting the DDA conditions using BrC filter extracts, a quality MS and MS/MS spectra were obtained for approx. 4000 features, which is comparable with similar, combustion-related samples (Brege et al., 2021; Divisekara et al., 2023; Young et al., 2021; Graham et al., 2002).

2.3 Mass spectrometric data processing workflows

The raw data files were first processed with MS-DIAL or MZmine (Fig. 2). First, the workflows based on MS-FINDER, CFM-ID, Metaboanalyst, GNPS, and MZmine were tested using 59 model compounds. These molecules were selected to mimic the molecular composition of water-soluble BrC emitted by BB based on previously published results and standards availability (Tables S1 and S2), and included derivatives of cinnamic acid, nitrophenols, and polycarboxylic, furoic, and fatty acids. The final workflow, used

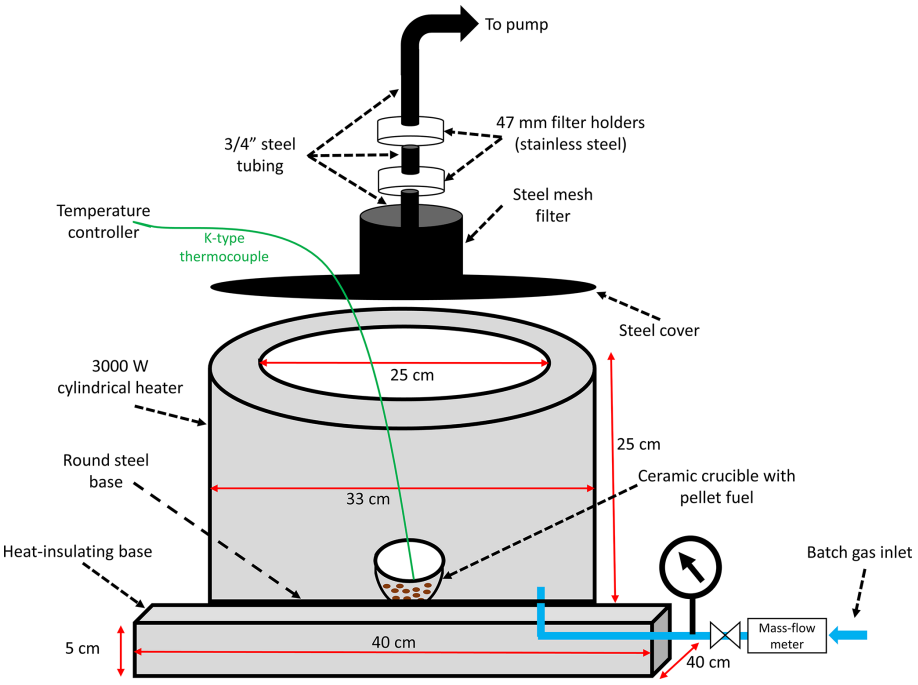

Figure 1. Diagram of the biomass combustor.

for analyzing BrC_{aq}, was based on MS-DIAL and MS-FINDER.

The same MS databases, including internal and user-uploaded libraries, were used in workflows based on MS-DIAL, MS-FINDER, and MZmine; GNPS allows user-defined databases, while the other web-based platforms (MetaboAnalyst and CFM-ID) are limited to pre-selected MS libraries – Table S6 (Lai et al., 2018; Vaniya et al., 2017; MoNa, 2024; MS-DIAL, 2024; Tsugawa et al., 2015). Workflows based on MZmine, GNPS, MetaboAnalyst, and CFM-ID are described in Sect. S3.1.

2.3.1 MS-DIAL

MS-DIAL (v5.3.240617) was used for the raw data processing, spectra deconvolution, and feature extraction and annotation – Fig. 3.

The identification criteria included retention time, precursor m/z, isotopic ratio, and MS/MS spectra (Fig. 3). MS/MS spectra were indispensable for feature annotation and distinguishing isomers. Here, the compound with the highest total score above 80 % was assigned to each focus peak (Tsugawa et al., 2015). In cases where DDA lacked MS/MS spectra, the MS/MS similarity value was zero, and the structure was proposed based on the MS1 score. The scoring approach implemented in MS-DIAL is described in more detail in Sect. S3.1.5).

The Microsoft Access Table (MAT) file, which included both MS and MS/MS spectra exported from MS-DIAL, was used as input data for MS-FINDER, CFM-ID, GNPS, and MetaboAnalyst but not MZmine (Fig. 2). Features not annotated by MS-DIAL were further analyzed using MS-FINDER (Sect. 2.3.2).

2.3.2 MS-FINDER

MS-FINDER v3.61 (Fig. 4) is a highly versatile tool for predicting formulas, annotating fragments, and elucidating structures. In addition to the internal libraries embedded in MS-FINDER, an in-silico MS/MS spectra predictor was used. Assigned structures were ranked based on their scoring.

In MS-FINDER, the formula candidates were considered based on mass error, isotopic ratio, product ions annotation, neutral-loss ions annotation, and database score (Fig. 4). Structural candidates were ranked using a weighted scoring system, integrating bond dissociation energies, mass similarities, fragment linkages, and, most importantly, nine hydrogen rearrangement rules during bond cleavages. The final molecular structure rankings were determined using a combined formula and structure scores (Tsugawa et al., 2016; Blaženović et al., 2018).

2.4 Confidence levels in annotation

Confidence levels in NTA are showcased in Table 1 (Schymanski et al., 2014).

For the features annotated at least level 4 (elemental formula assignment), the van Krevelen diagram, Kendrick mass defects, double-bound equivalents (DBE), and average car-

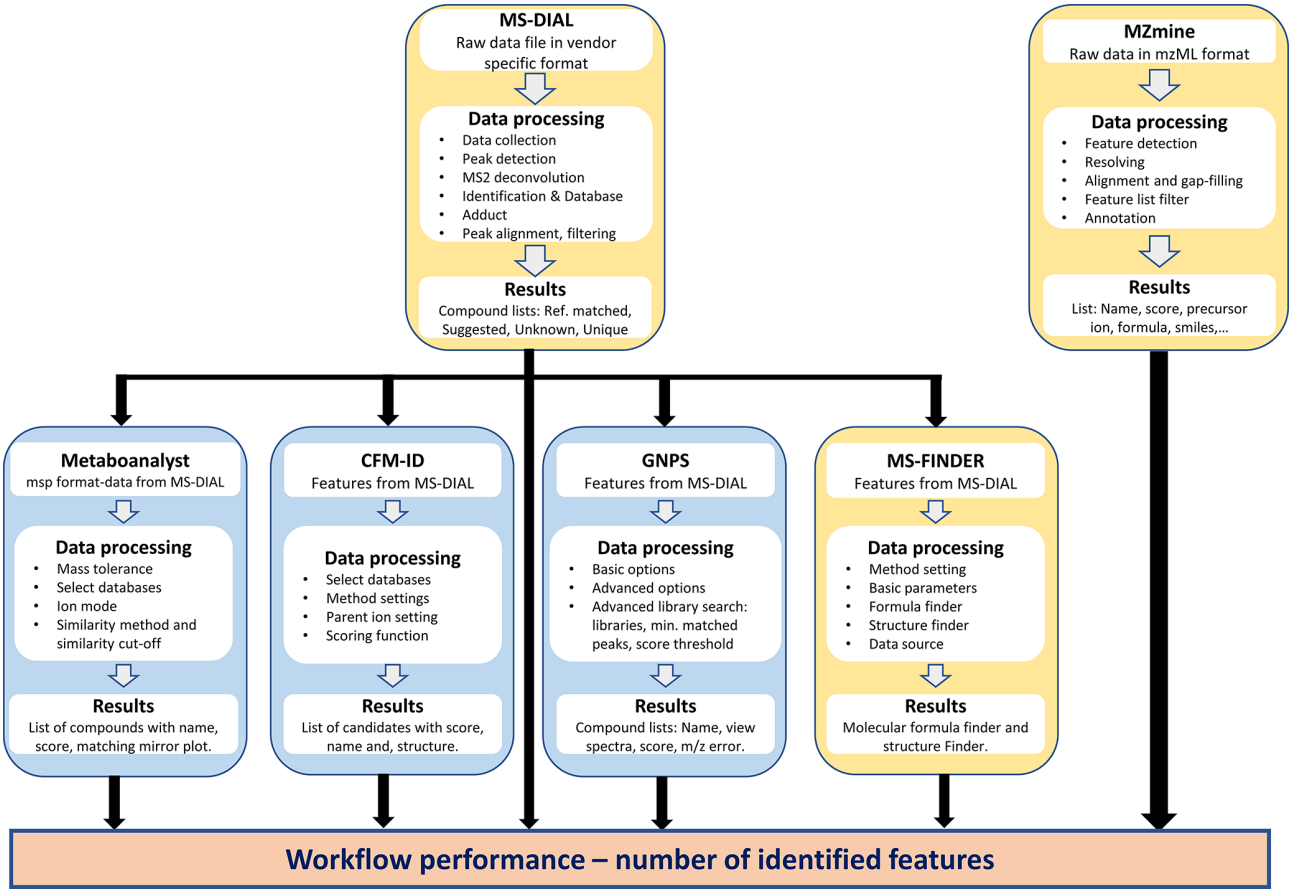

Figure 2. The MS data processing software was tested in this work. All data processing was performed with a Dell Vostro 3020T desktop PC equipped with an Intel Core i7-13700 CPU, 1TB SSD drive, and 64 GB of 3200 MHz DDR4 RAM.

Table 1. Confidence levels in the NTA workflow.

Confidence level	Required data	Classification	Description	Example
1	MS spectra, MS/MS spectra, library MS/MS spectra, and retention time matching	Confirmed with authentic standard	Input spectra matched with reference spectra by MS-DIAL with a retention time confirmation	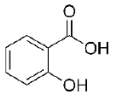
2	MS spectra, MS/MS spectra, library MS/MS spectra matching	Reference matched	Input spectra matched with reference spectra by MS-DIAL	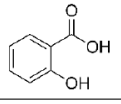
3	MS, MS/MS, experimental data	Suggested structure	From MS-DIAL, and MS-FINDER with MS/MS spectra	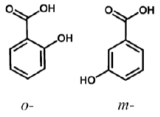 *o-* *m-*
4	MS isotope/adduct	Suggested formula	From MS-DIAL with MS spectra	$C_7H_6O_3$
5	MS	Unknowns	With MS spectra and an unknown compound with MS/MS spectra	m/z 137.0228

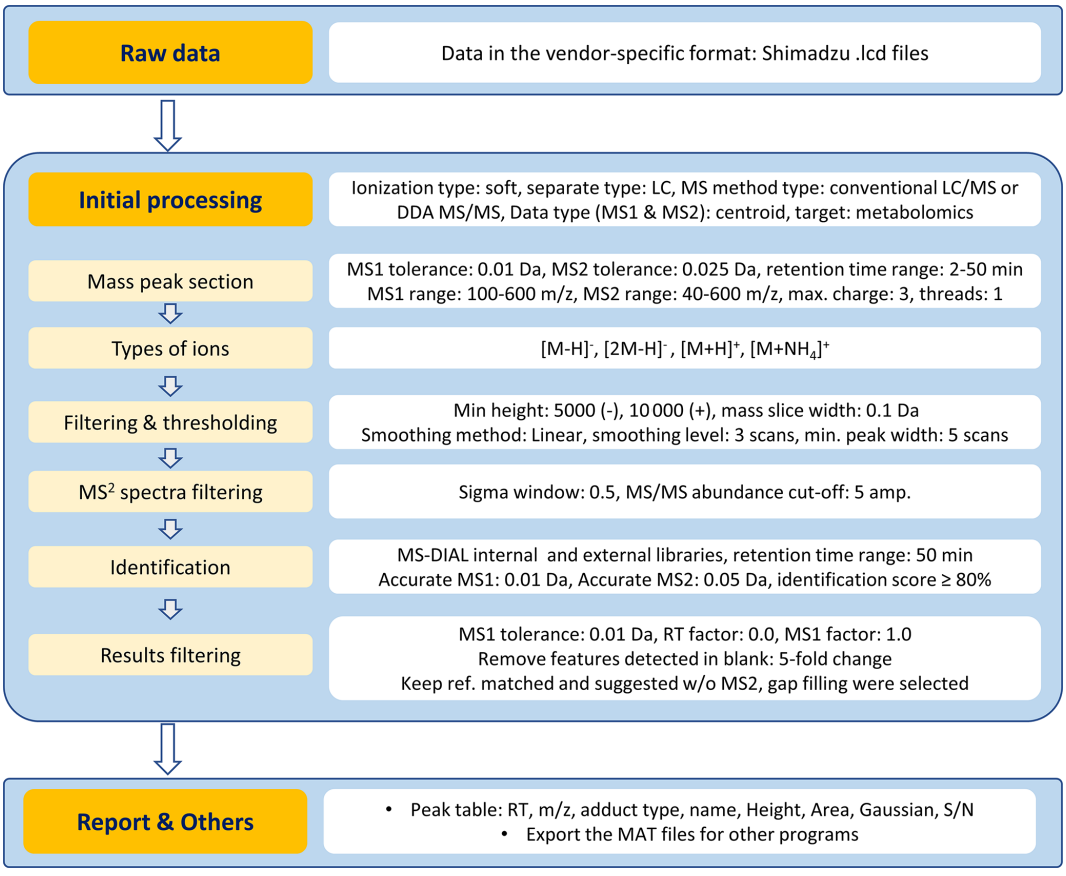

Figure 3. MS-DIAL workflow.

bon oxidation states (OS_c) were calculated – Sect. S4 (Kroll et al., 2011).

2.5 Semi-qualitative analyses with surrogate standards

Surrogate standards were used to quantify organic compounds detected in filter extracts; this approach assumes that closely eluting compounds have similar response factors (RFs) (Pieke et al., 2017). Five surrogate standards were used in each ionization mode, with retention times from 2 to 40 min (Table S3), covering the elution window for WSOCs detected in BrC_{aq}. Working standards were prepared in ($MeOH/H_2O$, 1 : 1, v/v) with concentrations from 0.001 to 0.05 mg L^{-1}.

RFs for surrogate standards were calculated with Eq. (1).

$$RF_{Surrogate} = \frac{A_{Surrogate}}{C_{Surrogate}} \quad (1)$$

In Eq. (1), $RF_{Surrogate}$ represents the ratio between the peak area $A_{Surrogate}$ and the concentration ($C_{Surrogate}$, mg L^{-1}) of the surrogate standards. The analyte concentrations were calculated using Eq. (2) (Pieke et al., 2017).

$$C_{unknown}\left(mg\,L^{-1}\right) = \frac{A_{unknown}}{RF_{closest\ surrogate}} \quad (2)$$

In Eq. (2), $RF_{closest\,ST}$ is the response factor of surrogate standards with the retention time closest to the analyte, and $A_{unknown}$ is the chromatographic peak area of the unknown compound. $C_{unknown}$ is the concentration of the analyte in mg L^{-1}. In Eq. (2), the total concentration of WSOCs in the filter extracts was calculated as the sum of concentrations of the individual analytes. Due to the use of surrogate standards, a 50 % uncertainty was imposed for all concentrations obtained with Eq. (2) (Kruve, 2019; Evans et al., 2024; Malm et al., 2021; Pieke et al., 2017). For compounds detected in BrC_{aq}, this value is consistent with the results obtained using authentic and surrogate standards (Table S4). Furthermore, the imposed 50 % uncertainty exceeds the matrix effects observed for most surrogate standards (Table S5). To prevent introducing a positive bias into the quantitative data, molecules detected in both ionization modes were identified by comparing annotation results, and their average concentrations were used to estimate the amount of BrC_{aq}.

The total (Σ_{LCMS}) and individual amounts of WSOCs emitted were derived with Eq. (3).

$$\Sigma_{LCMS}(g\,kg^{-1}) = \frac{\sum C_{unknown} \times DF \times V_{total}}{\Delta m_{fuel}} \quad (3)$$

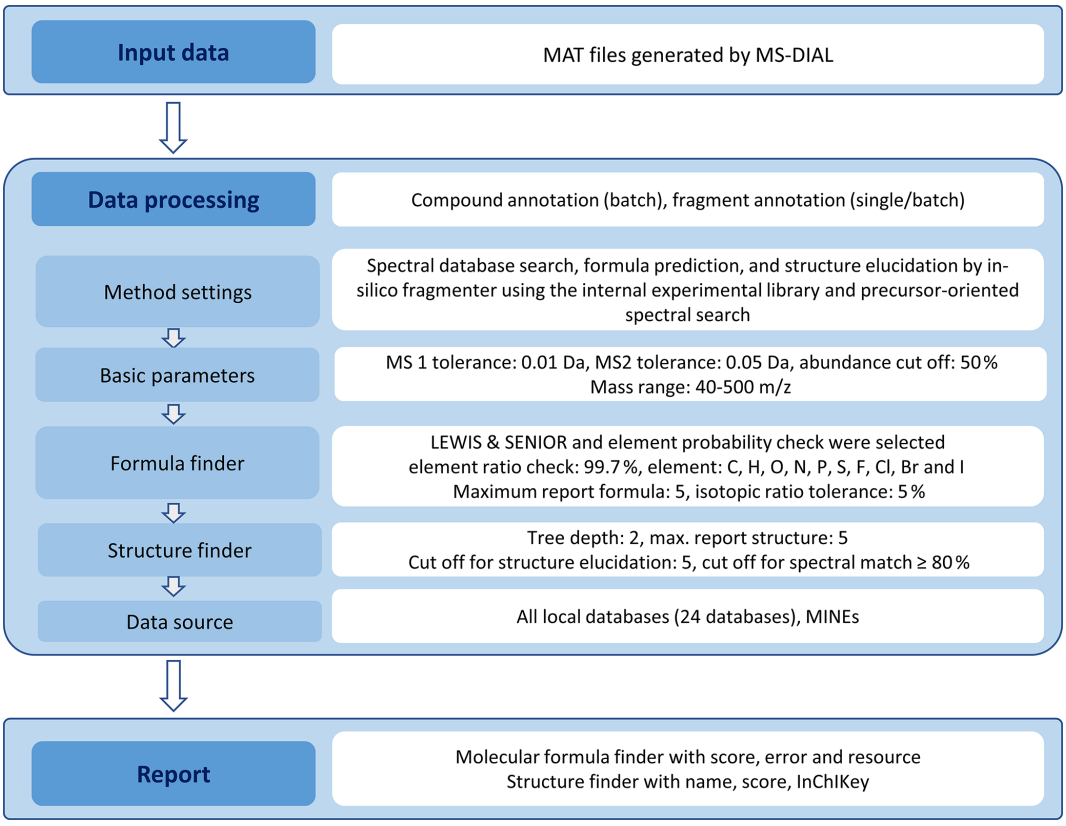

Figure 4. MS-FINDER workflow.

In Eq. (3), $\Sigma C_{\text{unknown}}$ is the sum of analytes (mg L^{-1}) from Eq. (2), DF is the dilution factor, V_{total} is the total volume of extraction solvent (2 mL), Δm_{fuel} is the decrease in the mass of pellets (g) corrected for the water content (8.0 %).

2.6 Total organic carbon analysis

Analyses were conducted using a Shimadzu TOC-5050A analyzer with an ASI-5000A autosampler. The instrument was calibrated with the standard solution of 4-nitrophenol and glucose between 4 and 40 (mg C L^{-1}). A squared linear coefficient of determination (R^2) of 0.9996 was obtained, and the RF values for the two standards were practically identical.

Samples were diluted with water to a ca. 20 mg C L^{-1} and filtered through a 0.22 µm PTFE syringe filter. Before injection, 50 μL^{-1} of 2 M HCl was added to each sample, followed by sparging with O_2 for 2 min. The injection volume was 21 µL, and each sample was injected three times, which yielded a precision < 1 %.

$$\Sigma_{\text{TOC}}(\text{g kg}^{-1}) = \frac{C_{\text{TOC}} \times \text{DF} \times V_{\text{total}}}{\Delta m_{\text{fuel}}} \times \frac{1}{0.625} \quad (4)$$

In Eq. (4), C_{TOC} is the measured concentration of TOC (mg C L^{-1}), DF is the dilution factor, V_{total} is the total volume of extraction solvent (2 mL), Δm_{fuel} is the fuel mass (g) corrected for the water content (8.0 %) and, 0.625 ± 0.144 (2σ) is the factor used to convert mg C L^{-1} units to mg L^{-1}. This conversion factor was the average carbon content of the analytes detected with LC-ToF/MS and the main source of the uncertainty of the TOC measurements.

2.7 Gravimetric analyses

Aqueous samples (0.4 mL) were filtered through a 0.22 µm PTFE filter and evaporated to dryness at 30 °C using a centrifugal vacuum evaporator (Labconco, model no. 7810033). Afterward, the dried residues were placed in a desiccator for 24 h to remove the leftover moisture. This procedure yielded ≥ 1 mg of residue, which was weighed using an analytical microbalance (Radwag, model no. XA52.5Y).

The amount of BrC_{aq} emitted was calculated with Eq. (5).

$$\text{TC}_{\text{grav}}(\text{g kg}^{-1}) = \frac{(m_{\text{residue}} - m_{\text{blank}}) \cdot V_{\text{total}}}{V_{\text{use}} \cdot \Delta m_{\text{fuel}}} \quad (5)$$

In Eq. (5), m_{residue} is the mass of the residue after evaporation (mg), m_{blank} is the mass of the blank (mg), V_{total} is the total volume of extraction solvent (2 mL), V_{use} is the volume of extract used for evaporation (0.4 mL), and Δm_{fuel} is the fuel mass (g) corrected for the water content (8.0 %).

2.8 Henry's law constants and toxicity estimates

Acute toxicity, measured as LD_{50} ($mg\,kg^{-1}$), was estimated using the VEGA-QSAR regression model (KNN, v. 1.0.0). Henry's Law values ($M\,atm^{-1}$) were estimated using OPERA, v.1.0.1 model (Mansouri et al., 2021; Mansouri et al., 2018).

Equations (6) and (7) were used to derive the total toxicity and H scores for individual compounds in BrC_{aq}.

$$H\ \text{score (arb)} = H \times \text{emission factor (LC/MS)} \quad (6)$$

$$LD_{50}\ \text{score (arb)} = \frac{1}{LD_{50}} \times \text{emission factor (LC/MS)} \quad (7)$$

Using Eqs. (6) and (7), the candidates for $_{aq}$SOAs precursors and the most harmful molecules, were identified by considering their properties and amounts emitted.

2.9 Quality and control measurements

Blank filters were prepared without the fuel (Sect. 2.1). The extract from the blank filter was then used to correct the TOC and LC-MS analysis results. After each experiment, the combustor was cleaned by heating the chamber to 550 °C and flushing with air ($5.0\,L\,min^{-1}$) for 1 h to oxidize the residues. The sampling assembly was sonicated in detergent, rinsed with distilled water and organic solvent, and dried in the oven.

3 Results and discussion

3.1 Non-target workflow selection

Workflows (Sects. 2.3 and S3.1) were evaluated using model compounds – Fig. 5.

The optimal workflow, combining MS-DIAL and MS-FINDER, correctly identified 73 % of standards (Fig. 2), similar to earlier studies (Young et al., 2021; Black et al., 2021). The combination of MS-DIAL and MS-FINDER also annotated 5 unique features not recognized by any other workflow, whereas MZmine annotated only one unique analyte – Fig. 5.

In addition to searching MS databases, MS-FINDER identifies unknown compounds using *silico* fragmentation algorithms (Blaženović et al., 2018). The performance of the combined workflow (Fig. 5) is attributed to the accurate prediction (simulation) of the fragmentation spectra in MS-FINDER (Tsugawa et al., 2016; Su et al., 2023). While MS-DIAL excelled in reproducibility and peak picking, MS-FINDER demonstrated a robust capability to identify unknown BB pollutants (Wartmann et al., 2024; Mallmann et al., 2023).

Despite using different peak-picking parameters (Figs. 3 and S1), the number of features extracted by MZmine and MS-DIAL was very similar. While MZmine extracted more features than MS-DIAL, it is not necessarily an indicator of higher data quality (Rivera-Pérez and Garrido Frenich,

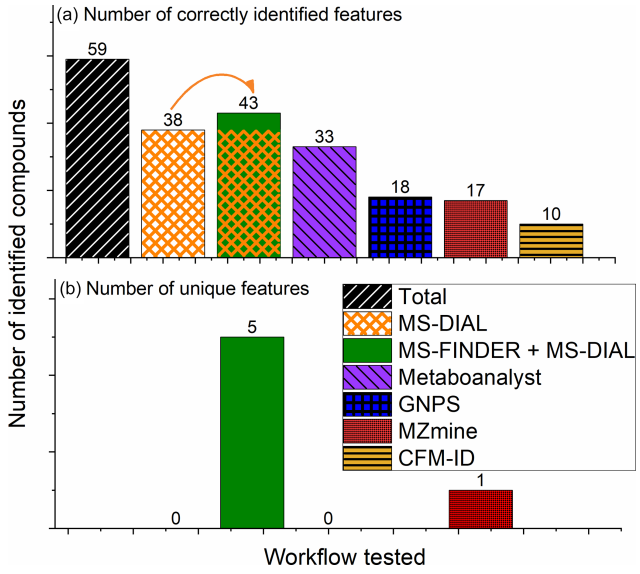

Figure 5. Workflow performance evaluation with the standard mixture of 59 model compounds (Table S1). Number of correctly identified analytes **(a)** and number of analytes identified only by a given software **(b)**.

2024). MZmine enhanced the accuracy with noise filter and duplicate peak filter (Heuckeroth et al., 2024), while MS-DIAL highlighted interference reduction using its "blank filtering" capability, currently absent in MZmine (Heuckeroth et al., 2024). These functions made MS-DIAL well-suited for NTA, further complemented by the user-friendly interface.

MZmine successfully identified only 29 % of standards, despite using the same databases as MS-DIAL and MS-FINDER (Table S6), consistent with earlier findings (Wartmann et al., 2024). Such a result is attributed to differences in mass peak-picking algorithms, which largely impacted the accuracy of extracted m/z values. In MZmine, mass detection was performed via the exact mass algorithm using the full width at half maximum paradigm to determine peak centers and extract m/z values and intensities (Hohrenk et al., 2020). On the other hand, MS-DIAL employed peak detection algorithms rooted in a linearly weighted smoothing average, regarding retention time and accurate mass (Tsugawa et al., 2014). This process was based on differential calculus principles and noise estimations, forming the backbone of MS-DIAL peak detection methodology (Tsugawa et al., 2015).

All web-based platforms, MetaboAnalyst, GNPS, and CFM-ID utilize measured and predicted spectra in their matching functions. MetaboAnalyst correctly identified 33 standards, while GNPS and CFM-ID identified only 18 and 10 out of 59 standards, respectively (Fig. 5).

In most MS data mining programs, MS/MS fragments are transformed into vectors. The cosine value, representing the angle between the input and reference vectors from

databases, is used to quantify their similarity (Li et al., 2021b). The MetaboAnalyst platform integrates similarity scores in a single value derived neither from the vector direction (dot-product) nor the vector magnitude (entropy) (Pang et al., 2024). In MS-DIAL, the similarity score is based on a combination of dot-product (also used in MetaboAnalyst) and secondary input spectra. The secondary input spectra remove fragments that did not appear in the reference spectra of the candidate compound. It decreases the impact of unwanted fragments derived from isotopic and background noise (Tsugawa et al., 2015). Consequently, for the selected standards (Sect. S1), the accuracy of the results generated by MS-DIAL and MetaboAnalyst is higher than the other tested programs (Fig. 5) (Tsugawa et al., 2015).

Databases embedded in CFM-ID contain nearly nine million spectra, but most are simulated (Table S6) (CFM-ID databases, 2024). Since CFM-ID identified only 10 standards (Fig. 5), the accuracy of these prediction algorithms was somewhat insufficient (Bremer et al., 2022). Another drawback of the CFM-ID is the requirement to provide three fragmentation spectra for each unknown compound, acquired at low, medium, and high CE to enhance the identification accuracy, which greatly prolongs the analysis time (Chao et al., 2020). Nevertheless, simulating MS/MS spectra with machine learning is a promising approach to identifying "known unknowns" via *in-silico* fragmentation and "unknown unknowns" in non-target identification (Bremer et al., 2022; Russo et al., 2024)

3.2 General characteristics of fine BrC_{aq}

The combined workflow (MS-DIAL and MS-FINDER) exhibited the best performance and was used to analyze the composition of BrC_{aq}. Analysis of BrC_{aq} yielded 4086 features; this number was reduced to 2121 features annotated at least at level 4 (elemental formula assignment, Table 1). These features were categorized based on their elemental composition – Fig. 6

The van Krevelen diagram (Fig. 6a) revealed the clustering of O/C and H/C ratios between 0.2–0.4 and 0.7–1.3, respectively, corresponding to molecules derived from lignins and tannins (D'Andrilli et al., 2015; Hartner et al., 2024), which were the most abundant in BrC_{aq}, both number and concentration-wise – Fig. 6 (Laszakovits and MacKay, 2021; Moschos et al., 2024). Similar results were previously reported for the ambient and chamber-generated BB aerosols (Fleming et al., 2018; Evans et al., 2025). Furthermore, a Kendrick Mass Defect plot (Fig. 6b) revealed a homolog series of CHON, CHO, and CHONS molecules with molecular weights between 150 and 300 Da, similar to organic aerosols emitted by dung and brushwood burning (Fleming et al., 2018).

Highly oxidized $C_xH_yO_{3-6}$ compounds with $C_xH_yO_4$ formulas were the most frequently detected, constituting 73 % of 96 annotated features detected with (−ESI). On the other hand, nitrogen-containing organic compounds, such as $C_xH_yNO_{2-4}$, and $C_xH_yN_z$, were predominantly observed in positive ion mode, accounting for approximately 38 % of all detected compounds – Fig. 6 (Ma et al., 2024; Li et al., 2024).

Double-bond equivalent (DBE) values (Fig. 6c), reflecting the degree of unsaturation, ranged from 4–6 for lignin pyrolysis products, 7–8 for coumarins, and 10–12 for stilbenes and flavonoids (Moschos et al., 2024; Koch and Dittmar, 2006). In Fig. 6c, 60 % of (−ESI) and 40 % of (+ESI) candidates fell within the potential BrC chromophores region, positioned between the lines for conjugated polyenes and linear fullerene-like hydrocarbons (Tang et al., 2020; Lin et al., 2018; Siemens et al., 2022; Moschos et al., 2024; Sun et al., 2024). The chromophore candidates were primarily lignin-like CHO molecules, followed by nitrogen-containing CHON compounds, previously identified in wood-burning BrC (Fleming et al., 2018; Evans et al., 2025).

The BrC_{aq} exhibited the carbon oxidation state (OS_c) values ranging from −2 to 1 (Fig. 6d), consistent with observations in organic aerosols within Earth's atmosphere (Moschos et al., 2024; Kroll et al., 2011). Furthermore, for approximately 83 % of the annotated compounds, the OS_c was between −2 and 0, characteristic of unaged emissions (Nihill et al., 2023). Hence, the general characteristics and oxidation state of BrC_{aq} corresponded to the unaged OAs emitted by BB (Moschos et al., 2024; Fleming et al., 2018; Smith et al., 2009; Song et al., 2018; Li et al., 2024).

3.3 Quantitative and qualitative analyses of fine BrC_{aq}

Quantitative analyses of the water-extractable fraction of fine BrC were performed with LC-MS using surrogate standards (Sect. 2.5), TOC (Sect. 2.6), and gravimetric analysis (Sect. 2.7) – Fig. 7.

The WSOCs detected in BrC_{aq} were classified as fatty and carboxylic acids, alkanes and aliphatic hydrocarbons, aromatic compounds, peptides, and polypeptides (Fig. 7) based on their general characteristics derived from elemental composition – Fig. 6 (Smith et al., 2009; Merel, 2023; Zherebker et al., 2024). BrC_{aq} was dominated by pyrolysis products of lignin and tannins, followed by lipids, peptides, hydrocarbons, condensed hydrocarbons, and carbohydrates (Seo et al., 2020; Shahid et al., 2019; Divisekara et al., 2023; Smith et al., 2020; Noblet et al., 2024; Hartner et al., 2024; Kawamoto, 2017).

An excellent agreement between the Σ_{LCMS}, Σ_{TOC}, and Σ_{grav} was obtained, but the first two values are largely implied by uncertainties – Fig. 7. Moreover, the values of Σ_{TOC} and Σ_{grav} may be affected by the loss of some volatile organics during sparging with O_2 (Sect. 2.6) and drying under vacuum (Sect. 2.7) and, such molecules were shown to contribute to BrC (Sinha et al., 2023; Priestley et al., 2024). Furthermore, the value of Σ_{grav} may include fine soot (not removed by the 0.22 µm filter, Sect. 2.7) and water-soluble inorganics, which can contribute 8.9 %–21 % to fine BrC (Ya-

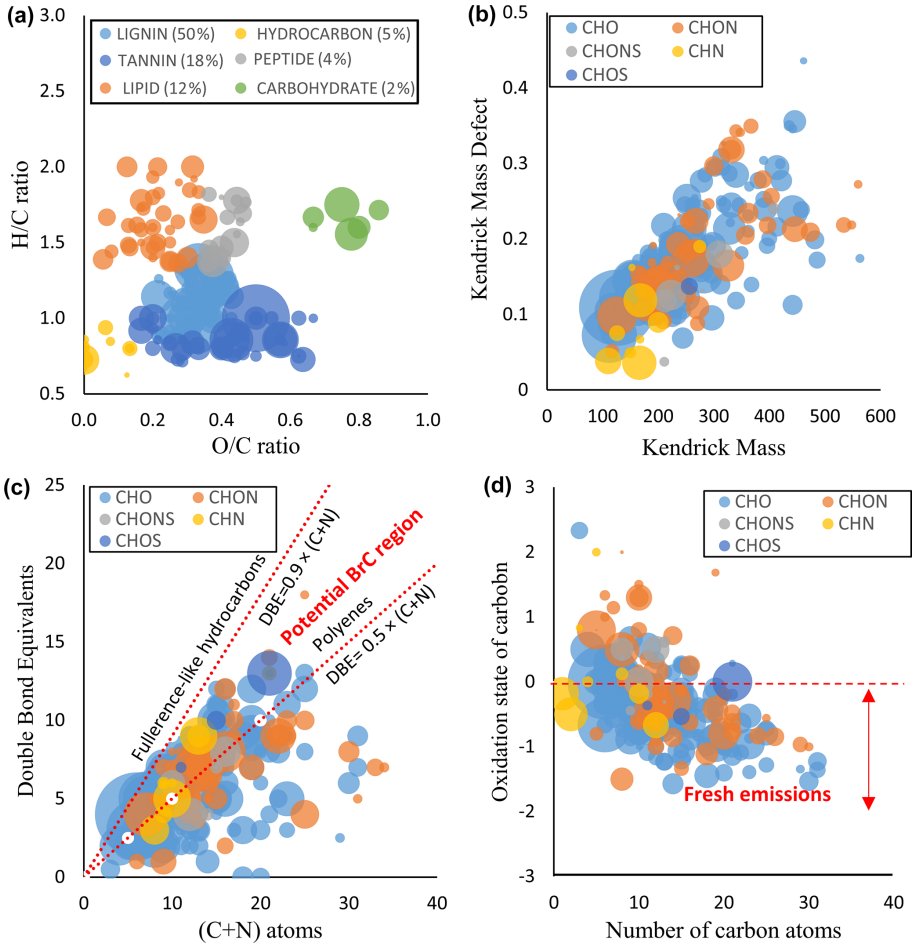

Figure 6. The van Krevelen Diagram **(a)**, Kendrick Mass Defect **(b)**, DBE vs. (C + N) atoms **(c)**, and OS_c vs. C atoms **(d)** plots for unique molecular compounds of water-soluble particulate matter identified by MS-DIAL and MS-FINDER. The combination of symbols C, H, O, N, and S refers to the molecules composed of the listed elements. The size of the circles corresponds to the relative concentrations in the aqueous extracts obtained with LC/MS using surrogate standards (Sect. 2.5). These general characteristics (Sect. S4) of water-extractable BrC were comparable to those of the surrogate standards used to evaluate the NTA workflows (Table S2).

dav et al., 2023; Trubetskaya, 2022). Nevertheless, the results (Fig. 7) indicate that the semi-qualitative analysis with LC/MS (Sect. 2.5) reasonably estimated the total concentration of BrC_{aq} (Seo et al., 2020; Shahid et al., 2019; Divisekara et al., 2023; Smith et al., 2020; Noblet et al., 2024; Hartner et al., 2024; Evans et al., 2024).

The total emission of polar, water-soluble organics from wood pyrolysis at 350 °C, representing the (oxygen-depleted) smoldering conditions, was ca. 1 g kg^{-1} of fuel burned (Fig. 7). The values derived for individual WSOCs (mg kg^{-1}) were derived with Eq. (3) (Sect. 2.5) pertains solely to the water-soluble fraction of fine BrC and should be regarded as a rough estimate of the actual emission factors (EFs) (Pokhrel et al., 2021). Nevertheless, the amounts of individual WSOCs emitted (Tables S8 and S9) are comparable with the EFs (mg kg^{-1}) range reported for the minor BB pollutants, including semi-volatile organics (Akagi et al., 2011), indicating a significant contribution of water-soluble organics to BB emissions.

3.4 Molecular composition and properties of the fine, water-soluble brown carbon

The BrC_{aq} sampled from the combustor was analyzed in DDA mode, and the detected features were annotated by MS-DIAL and MS-FINDER – Fig. 8.

The extracted features were first annotated at level 4 (elemental formula assignment) based on the MS1 spectra. At this stage, 51 % (-ESI) and 20 % (+ESI) of features were denoted as unknowns – Fig. 8. Subsequently, MS2 spectra were further analyzed, and 12 % (−ESI) and 59 % (+ESI) of total features were annotated at least at level 3. Furthermore, confidence level 4, or higher, was obtained for 44 % and 80 % of the detected features in negative and positive ionization modes, respectively (Yang et al., 2023; Schymanski

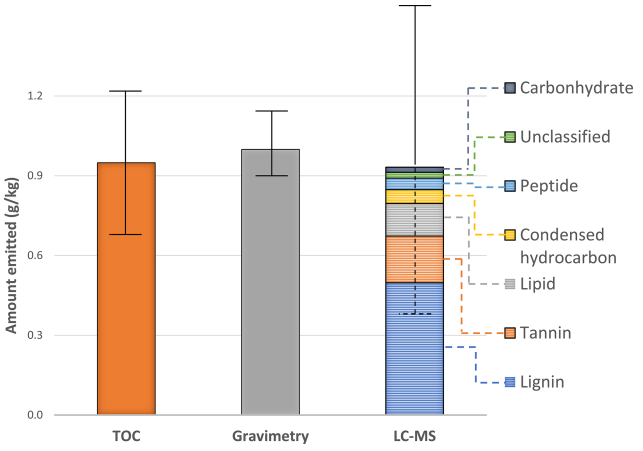

Figure 7. The total concentration of BrC_{aq} (PM3) generated by pyrolysis of wood pellets at 350 °C measured with LC-MS (Σ_{LCMS}), TOC (Σ_{TOC}), and gravimetry (Σ_{grav}). The data presented are provided in Table S10.

et al., 2014). MS databases for positive ion mode contained over 326 000 records compared to 53 337 records in negative mode (Table S6), which likely enhanced the annotation results for (+ESI) – Fig. 8 (Ng, 2021). Hence, the database plays a critical role in the structural elucidation of NTA, but currently, the number of (freely available) MS/MS databases focused on environmental pollutants is limited (Ng, 2021).

Major WSOCs detected in BrC_{aq} were tentatively identified using NTA – Fig. 9.

The major tracers of BB identified include phenols and methoxyphenols originating from lignin and tannin pyrolysis (Fig. 9a–b) (Li et al., 2021a; Hartner et al., 2024; Wan et al., 2019). As previously reported, products derived from aromatic alcohols sinapyl, coniferyl, and p-coumaryl constituted 53.4 % of WSOCs generated by the combustion of lignin (Fleming et al., 2018; Kawamoto, 2017; Simoneit, 2002). Furthermore, mono and poly-carboxylic acids, including succinic, glutaric, adipic, sorbic, and azelaic acids (Hu and Yu, 2013; Narukawa et al., 1999), were identified as major compounds in the lipid fraction (Fig. 9c), consistent with the polar semi-volatile organic compounds from laboratory-generated BB emissions and fine particles collected at an urban location (Sengupta et al., 2020; Hu and Yu, 2013; Shen et al., 2022). Condensed aromatics and hydrocarbons, peptides, and carbohydrates were minor components of BrC_{aq} (Fig. 9d–f). While some studies reported higher emissions of these molecules, their contribution varies considerably depending on the pyrolysis temperature (Zhang et al., 2024; Oros et al., 2006; Chang et al., 2024).

Structures of 361 out of the 420 WSOCs detected in BrC_{aq} were tentatively identified for the first time (Tables S8 and S9). Of the 50 most abundant molecules in BrC_{aq} (Table S11) identified at least at level 3 (Table 1), 28 % were previously detected in ambient and laboratory-generated (light-absorbing) OAs (Yee et al., 2013; Sengupta et al., 2020; Divisekara, 2023; Moschos et al., 2024; Fleming et al., 2020; Oros et al., 2006; Graham et al., 2002; Hartner et al., 2024; Bianco et al., 2016; Oros and Simoneit, 2001; Chan et al., 2020).

These (newly) identified structures were used to estimate H and LD_{50} values (Sect. 2.8) listed in Tables S12 and S13. The estimated properties exhibited almost no correlation with the elemental composition and the general characteristics of WSOCs annotated at least at level 4 (Table 1), including the number of O, N, C, and S atoms and N/O ratio for each molecule (Table S14). Statistically significant (p value < 0.05), but weak ($r = 0.561$) correlation was observed between H values and the number of oxygen atoms. Hence, the properties of polar (complex) molecules in BrC_{aq} cannot be even roughly constrained using simple parameters derived from HR-MS measurements, and more sophisticated models, such as quantitative structure-activity relationships (QSARs), are necessary (Mansouri et al., 2021; Mansouri et al., 2018).

3.5 Potential precursors of $_{aq}$SOAs in fine BrC_{aq}

Because some structural assignments were ambiguous, which is inevitable in NTA (Hulleman et al., 2023; Hohrenk et al., 2020), the list of potential $_{aq}$SOAs precursors with the 50 highest H scores (Table S12) was further refined – Fig. 10.

The newly identified $_{aq}$SOAs precursor candidates included cyclic and aromatic acids and esters, which can be classified as typical BB tracers (Fig. 10a) (Laskin et al., 2025; Wan et al., 2019). Furthermore, relatively large quantities of natural compounds present in roots and leaves (Fig. 10b), and natural dyes, including flavonoids (aglycones and glucosides, Fig. 10c) and anthraquinones (Fig. 10d), and coumarins (Fig. 10e) were also identified (Lin et al., 2016; Moschos et al., 2024; Laskin et al., 2025; Huang et al., 2022). In addition to high solubility in water, natural dyes substantially contribute to the BrC absorption between 300 and 370 nm (Laskin et al., 2025; Zhou et al., 2021). Moreover, one diterpenoid (Fig. 10e) and several fungal and bacterial metabolites (Fig. 10g and h) were detected (Laskin et al., 2025; Wei et al., 2019).

Molecules shown in Fig. 10 (or their analogs) can be obtained from commercial suppliers and serve as model precursors for investigating the combustion-related $_{aq}$SOAs. To date, such studies have focused primarily on (nitrated) phenols (Lei et al., 2025; Jiang et al., 2021; Hems and Abbatt, 2018; Witkowski et al., 2022). Hence, studying these newly identified WSOCs can shed new light on the formation and evolution of light-absorbing OAs in the atmospheric hydrometeors, even if they only serve as proxies of ambient BrC (Hems et al., 2020; Liu et al., 2020; Laskin et al., 2025). The atmospheric lifetimes of the compounds shown in Fig. 10 due to the reaction with OH (the major daytime atmospheric oxidant) are further discussed in Sect. 4.

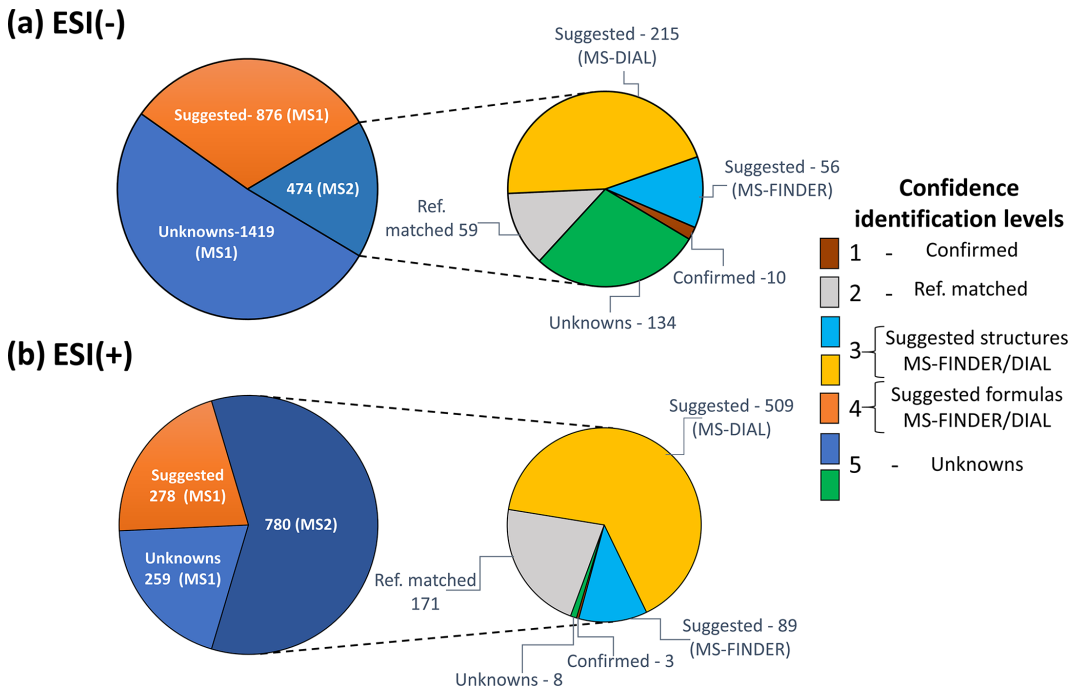

Figure 8. The number of features extracted and identified by MS-DIAL and MS-FINDER in fine BrC generated by pyrolysis of woody biomass at 350 °C; negative **(a)** and positive **(b)** ionization modes. All compounds identified in both ionization modes are listed in Tables S8 and S9.

3.6 Toxic compounds identified in fine BrC_{aq}

The newly identified molecules with the highest LD_{50} scores (Table S13) are shown in Fig. 11.

Of the 50 WSOCs with the highest LD_{50} scores, 32 were classified as moderately ($50 < LD_{50} < 500$) toxic, and harmful ($500 < LD_{50} < 2000$), with five highly toxic ($LD_{50} < 50$) molecules – Table S13 (Gadaleta et al., 2019). Several N-containing compounds were identified among the toxic components of BrC_{aq} (Fig. 11) (Pflieger and Kroflič, 2017; Majewska et al., 2021). However, no correlation of the LD_{50} values with the number of N atoms or N/O ratios (Table S14) underscores that such general classifications can be unreliable and more sophisticated methods are needed to evaluate whether or not a given pollutant is harmful (Young et al., 2021; Khan et al., 2021). The newly identified WSOCs included natural compounds (Fig. 11a), particularly alkaloids (Fig. 11b), which were seldom identified as (harmful) BB tracers (Young et al., 2021; Nizkorodov et al., 2011).

Furthermore, plant and wood care products (Fig. 11c) and fungal metabolites (Fig. 11d) were detected in a toxic fraction of BrC_{aq} (Laskin et al., 2025; Wei et al., 2019; Růžičková et al., 2021). The release of insecticides from commercial pellet fuel was previously observed at low-temperature pyrolysis (here, 350 °C was used – Sect. 2.1), which is insufficient to decompose such molecules (Růžičková et al., 2021). Forest protection with man-made chemicals and the production of wood pellets from different waste materials contribute to releasing these toxic WSOCs (Růžičková et al., 2021; Cesprini et al., 2021; Alakoski et al., 2016). Furthermore, the raw material for wood pellets usually contains between 70 % and 95 % tree wood and thus can include other kinds of forest biomass (Cesprini et al., 2021), but secondary contamination during storage (e.g., fungal growth) is also possible (Alakoski et al., 2016). In vegetation fires, properties cannot be controlled, but the current wood pellet quality standards do not consider the organic (micro)pollutants (Cesprini et al., 2021; Alakoski et al., 2016).

3.7 Atmospheric implications

The chemical aging of BB aerosols is connected with the formation and evolution (bleaching) of BrC (Wong et al., 2019; Zhao et al., 2015; Choudhary et al., 2023; Witkowski et al., 2022). Therefore, the lifetimes of potential $_{aq}$SOA precursors shown in Fig. 10 due to reaction with OH were estimated with Eq. (8) (Sarang et al., 2021).

$$\tau = \frac{1}{\left(\frac{k_{OH_{gas}}}{H^{cc}_{OH}} + k_{OH_{aq}} H^{cc}_{BrC} \omega\right) [OH]_{aq}} \quad (8)$$

In Eq. (8), τ is the overall gas and aqueous phase lifetime due to the reaction with OH. The equilibrium concentrations of individual BrC_{aq} and OH in both phases are derived using the dimensionless H^{cc}_{OH} and H^{cc}_{BrC} values (Sander, 2015), and

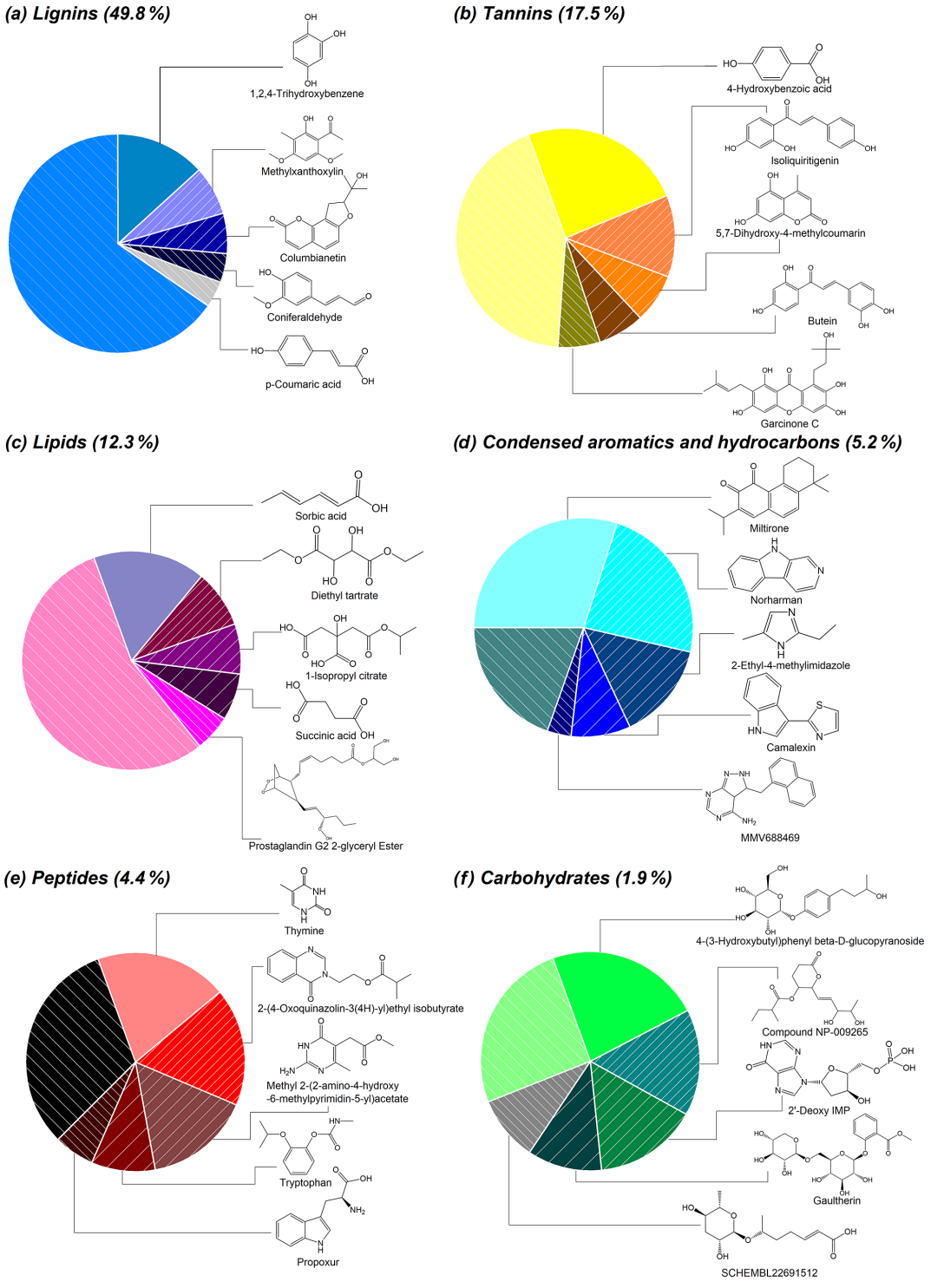

Figure 9. Tentatively assigned structures of the most abundant WSOCs in BrC_{aq}, classified as derivatives and pyrolysis products of lignins **(a)**, tannins **(b)**, lipids **(c)**, condensed aromatics and hydrocarbons **(d)**, peptides **(e)**, and carbohydrates **(f)**. Detected compounds were assigned to these groups based on assigned elemental formulas (confidence level 4 in Table 1) as presented in Fig. 6. Unlabeled areas correspond to unidentified molecules in each group. Only five major components from each group are shown, and all structural assignments via NTA and identification confidence levels 1 to 3 are listed in Tables S8 and S9.

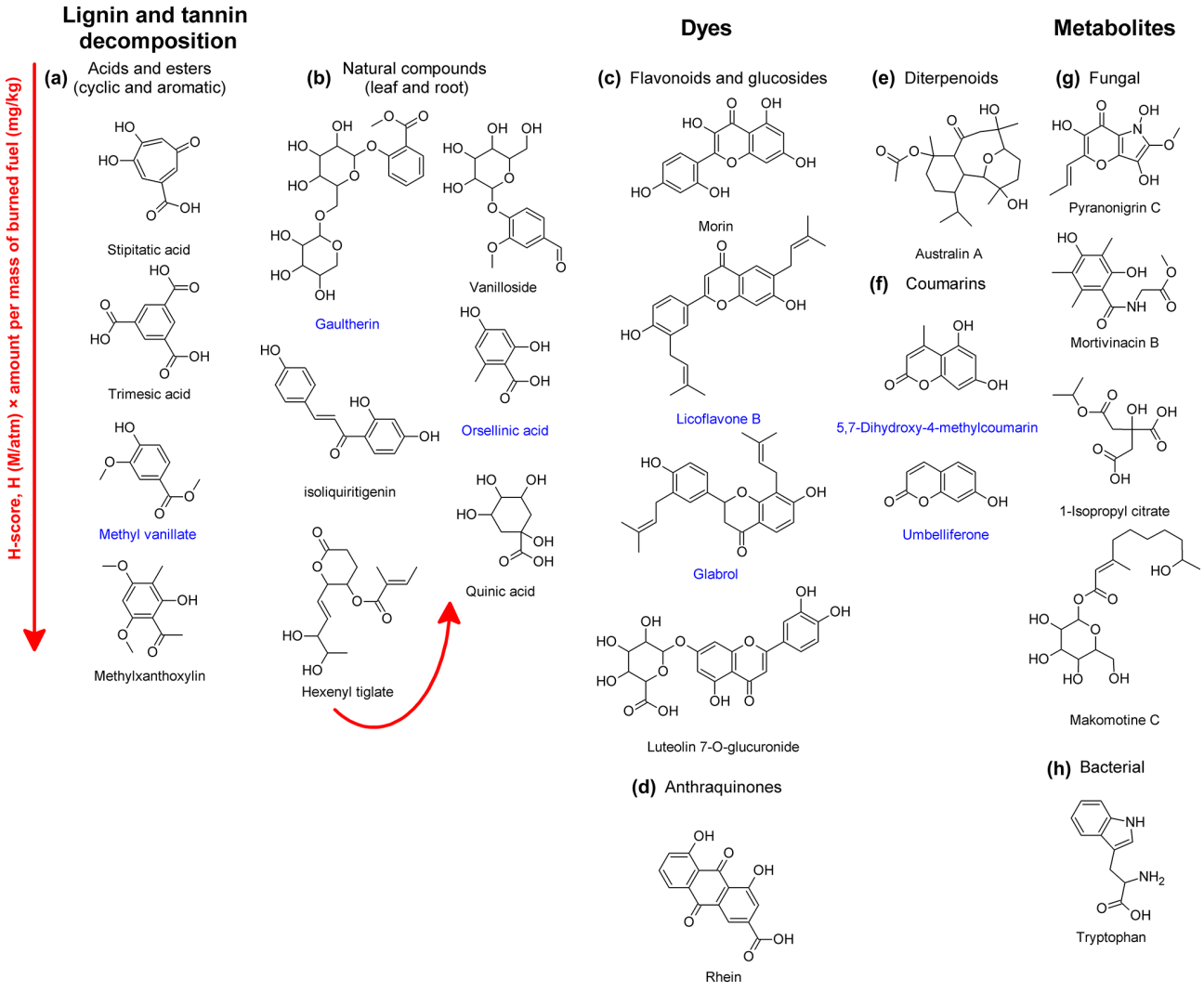

Figure 10. Newly identified potential precursors of $_{aq}$SOAs with the highest H scores (Eq. 6 in Sect. 2.8). The structures shown were assigned at levels 2 and 3, with names shown in black and blue, respectively. Identification levels in NTA are showcased in Table 1; the lower is better. Seven out of twenty-two compounds shown were identified at the 2nd level, the highest possible confidence without using authentic standards.

liquid water content (LWC, ω, unit $m^3\ m^{-3}$). The bimolecular reaction rate coefficients ($k_{OH_{gas}}$, and $k_{OH_{aq}}$ – Table S15) at 298K were estimated with *py*SiRC model (Sanches-Neto et al., 2021).

The lifetimes estimated with Eq. (8) for the potential precursors of $_{aq}$SOAs (Fig. 10) cover a wide range of values from less than 1 min to several hours – Fig. 12a.

Considering the aqueous processing of BB emissions in the atmosphere, continental (urban and remote) cloud-water processing is the most relevant, with marine scenarios being feasible following long-range transport (Che et al., 2022; Laskin et al., 2025). The τ values for all compounds with high H scores (Table S12) were affected by liquid water even in urban clouds, with the lowest $[OH]_{aq}$ (Fig. 12a). An estimated time of air-parcel interaction with the cloud is very long (18 h) (Herrmann et al., 2015), but the cloud droplet lifetimes are < 1 min (Kumar et al., 2013; Paulson et al., 2019). The estimated τ values also do not consider aqueous sources of OH, primarily Fenton (like) reactions, which can increase $[OH]_{aq}$ by several orders of magnitude (Kuang et al., 2020; Paulson et al., 2019).

Under these assumptions, of all potential precursors (Table S12), the most reactive molecules and those emitted in the highest quantities were selected (Fig. 12b). Thus, these newly identified WSOCs (Fig. 10) will likely undergo aqueous OH oxidation under realistic atmospheric conditions. Analyzing the yields of $_{aq}$SOAs from these precursors would require a separate investigation. However, compounds with large carbon backbones (Fig. 10) will likely yield low-volatility products following a reaction with OH

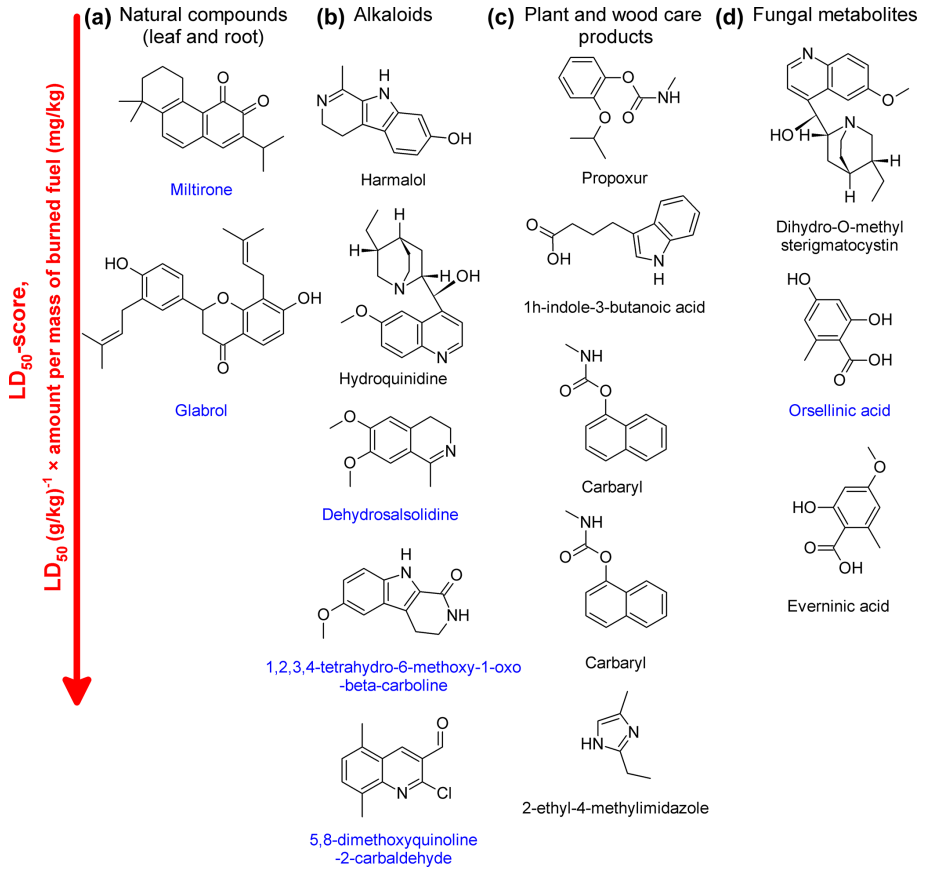

Figure 11. Newly identified, harmful components of BrC_{aq} with the highest LD_{50} scores (Eq. 7 in Sect. 2.8). The structures shown were assigned at levels 2 and 3, with names shown in black and blue, respectively. Identification levels in NTA are showcased in Table 1; the lower is better. Six out of fifteen compounds shown were identified at the 2nd level, the highest possible confidence without using authentic standards.

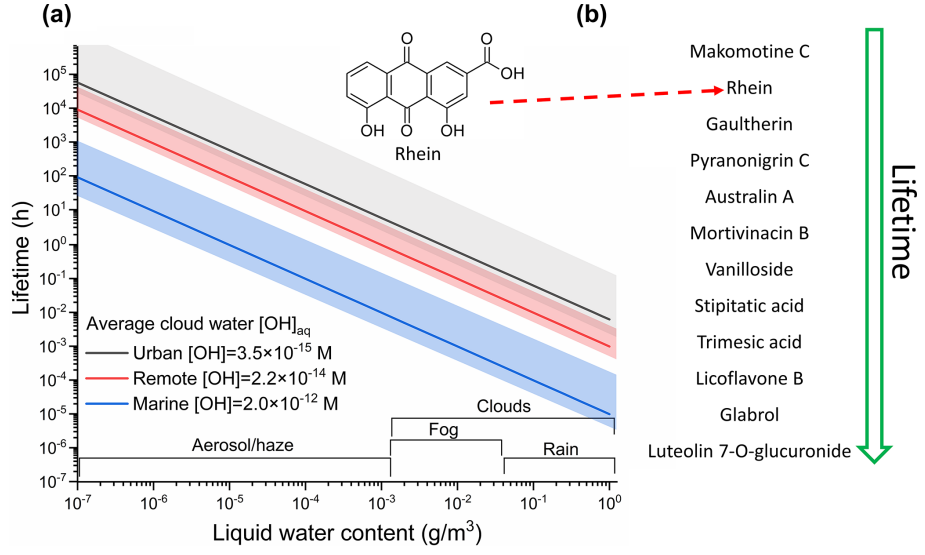

Figure 12. **(a)** estimated τ values (Eq. 8) for anthraquinone rhein due to the reaction with OH in different atmospheric hydrometeors, shaded areas represent the highest and lowest $[OH]_{aq}$. Only one sample plot is shown because the same profiles were obtained for all compounds listed in Table S12 (molecules with the highest H scores). **(b)** the potential precursors of $_{aq}$SOAs with the shortest lifetimes are listed.

without decomposing, at least during the early stages of oxidation (Fig. 12) (Herraiz and Galisteo, 2015).

4 Conclusions

This work revealed new, water-soluble tracers of wood combustion in fine, water-soluble BrC, including insecticides, wood-care products, and bacterial and fungal metabolites. The release of these compounds is possible during vegetation fires and domestic uses of wood and pellet fuel, contributing to the adverse health effects of open and domestic BB. Furthermore, in the case of vegetation fires, even 70 % of the fuel is consumed under oxygen-depleted and smoldering conditions (Akagi et al., 2011), likely favoring the release of polar, water-soluble organics, such as the molecule newly identified in this work (Chen and Bond, 2010). Global, annual emissions from open BB (not including domestic uses) were estimated at ca. 2600 Tg C, including 18.6 Tg of particle-bound organic carbon (Liu et al., 2024). At the same time, very little data is still available about the EF of the polar, higher-molecular-weight WSOCs emitted by open BB, even though such molecules are released during combustion and pyrolysis without decomposing (Li et al., 2021a). This work revealed that the amount of water-soluble organics emitted under oxygen-depleted conditions may be comparable to the EFs of non-polar, lower-molecular-weight BB tracers. Such molecules can form light-absorbing SOAs following oxidation reactions in different hydrometeors and contribute to the adverse health effects of BB emissions.

Studying the light-absorbing properties of BrC_{aq} was beyond the scope of this work; however, new potential chromophores, including natural dyes and molecules with conjugated double bonds and aromatic rings, were also identified (Tables S8–S9). The results presented provide new insights into the structures of BrC chromophores (Laskin et al., 2025).

Data availability. The raw data can be obtained by contacting the corresponding author.

Supplement. The supplement related to this article is available online at https://doi.org/10.5194/acp-25-10965-2025-supplement.

Author contributions. BW designed the study, developed the methodology, and analyzed the data. VN carried out the experiments, optimized the methodology, and processed the raw data. TG supervised the experiments, analyzed the data. All authors contributed to the interpretation of the results and contributed to manuscript writing and editing.

Competing interests. The contact author has declared that none of the authors has any competing interests.

Disclaimer. Publisher's note: Copernicus Publications remains neutral with regard to jurisdictional claims made in the text, published maps, institutional affiliations, or any other geographical representation in this paper. While Copernicus Publications makes every effort to include appropriate place names, the final responsibility lies with the authors. Also, please note that this paper has not received English language copy-editing.

Acknowledgements. This work was carried out at the Biological and Chemical Research Centre, University of Warsaw, established within the project co-financed by the European Union from the European Regional Development Fund under the Operational Programme Innovative Economy, 2007–2013. We thank the anonymous reviewers for their insightful comments and suggestions that helped to enhance the scientific quality of this article.

Financial support. This project was funded by the Polish National Science Centre (grant no. 2021/43/B/ST10/00931).

Review statement. This paper was edited by Ryan Sullivan and reviewed by two anonymous referees.

References

Admasie, A., Kumie, A., and Worku, A.: Children under Five from Houses of Unclean Fuel Sources and Poorly Ventilated Houses Have Higher Odds of Suffering from Acute Respiratory Infection in Wolaita-Sodo, Southern Ethiopia: A Case-Control Study, J. Environ. Public Health., 2018, 9320603, https://doi.org/10.1155/2018/9320603, 2018.

Akagi, S. K., Yokelson, R. J., Wiedinmyer, C., Alvarado, M. J., Reid, J. S., Karl, T., Crounse, J. D., and Wennberg, P. O.: Emission factors for open and domestic biomass burning for use in atmospheric models, Atmos. Chem. Phys., 11, 4039–4072, https://doi.org/10.5194/acp-11-4039-2011, 2011.

Alakoski, E., Jämsén, M., Agar, D., Tampio, E., and Wihersaari, M.: From wood pellets to wood chips, risks of degradation and emissions from the storage of woody biomass – A short review, Renew. Sustain. Energy Rev., 54, 376–383, https://doi.org/10.1016/j.rser.2015.10.021, 2016.

Amegah, A. K. and Jaakkola, J. J.: Household air pollution and the sustainable development goals, Bull. World Health Org., 94, 215–221, https://doi.org/10.2471/blt.15.155812, 2016.

Andreae, M. O.: Emission of trace gases and aerosols from biomass burning – an updated assessment, Atmos. Chem. Phys., 19, 8523–8546, https://doi.org/10.5194/acp-19-8523-2019, 2019.

Antar, M., Lyu, D., Nazari, M., Shah, A., Zhou, X., and Smith, D. L.: Biomass for a sustainable bioeconomy: An overview of world biomass production and utilization, Renew. Sustain. Energy Rev., 139, 110691, https://doi.org/10.1016/j.rser.2020.110691, 2021.

Aron, A. T., Gentry, E. C., McPhail, K. L., Nothias, L.-F., Nothias-Esposito, M., Bouslimani, A., Petras, D., Gauglitz, J. M., Sikora, N., Vargas, F., van der Hooft, J. J. J., Ernst, M., Kang, K. B., Aceves, C. M., Caraballo-Rodríguez, A. M., Koester, I., Weldon, K. C., Bertrand, S., Roullier, C., Sun, K., Tehan, R. M.,

Boya P, C. A., Christian, M. H., Gutiérrez, M., Ulloa, A. M., Tejeda Mora, J. A., Mojica-Flores, R., Lakey-Beitia, J., Vásquez-Chaves, V., Zhang, Y., Calderón, A. I., Tayler, N., Keyzers, R. A., Tugizimana, F., Ndlovu, N., Aksenov, A. A., Jarmusch, A. K., Schmid, R., Truman, A. W., Bandeira, N., Wang, M., and Dorrestein, P. C.: Reproducible molecular networking of untargeted mass spectrometry data using GNPS, Nat. Protoc., 15, 1954–1991, https://doi.org/10.1038/s41596-020-0317-5, 2020.

Bellouin, N., Quaas, J., Gryspeerdt, E., Kinne, S., Stier, P., Watson-Parris, D., Boucher, O., Carslaw, K. S., Christensen, M., Daniau, A.-L., Dufresne, J.-L., Feingold, G., Fiedler, S., Forster, P., Gettelman, A., Haywood, J. M., Lohmann, U., Malavelle, F., Mauritsen, T., McCoy, D. T., Myhre, G., Mülmenstädt, J., Neubauer, D., Possner, A., Rugenstein, M., Sato, Y., Schulz, M., Schwartz, S. E., Sourdeval, O., Storelvmo, T., Toll, V., Winker, D., and Stevens, B.: Bounding Global Aerosol Radiative Forcing of Climate Change, Rev. Geophys., 58, e2019RG000660, https://doi.org/10.1029/2019RG000660, 2020.

Bianco, A., Passananti, M., Deguillaume, L., Mailhot, G., and Brigante, M.: Tryptophan and tryptophan-like substances in cloud water: Occurrence and photochemical fate, Atmos. Environ., 137, 53–61, https://doi.org/10.1016/j.atmosenv.2016.04.034, 2016.

Black, G. P., He, G., Denison, M. S., and Young, T. M.: Using Estrogenic Activity and Nontargeted Chemical Analysis to Identify Contaminants in Sewage Sludge, Environ. Sci. Technol., 55, 6729–6739, https://doi.org/10.1021/acs.est.0c07846, 2021.

Blaženović, I., Kind, T., Ji, J., and Fiehn, O.: Software Tools and Approaches for Compound Identification of LC-MS/MS Data in Metabolomics, Metabolites, 8, 31, https://doi.org/10.3390/metabo8020031, 2018.

Brege, M. A., China, S., Schum, S., Zelenyuk, A., and Mazzoleni, L. R.: Extreme Molecular Complexity Resulting in a Continuum of Carbonaceous Species in Biomass Burning Tar Balls from Wildfire Smoke, ACS Earth Space Chem., 5, 2729–2739, https://doi.org/10.1021/acsearthspacechem.1c00141, 2021.

Bremer, P. L., Vaniya, A., Kind, T., Wang, S., and Fiehn, O.: How well can we predict mass spectra from structures? Benchmarking competitive fragmentation modeling for metabolite identification on untrained tandem mass spectra, J. Chem. Inf. Model., 62, 4049–4056, 2022.

Cesprini, E., Greco, R., Causin, V., Urso, T., Cavalli, R., and Zanetti, M.: Quality assessment of pellets and briquettes made from glued wood waste, Eur. J. Wood Wood Prod., 79, 1153–1162, https://doi.org/10.1007/s00107-021-01695-1, 2021.

CFM-ID ESI-MS/MS database description and statistics, https://cfmid.wishartlab.com/statistics (last access: 26 November 2024), 2024.

Chan, L. K., Nguyen, K. Q., Karim, N., Yang, Y., Rice, R. H., He, G., Denison, M. S., and Nguyen, T. B.: Relationship between the molecular composition, visible light absorption, and health-related properties of smoldering woodsmoke aerosols, Atmos. Chem. Phys., 20, 539–559, https://doi.org/10.5194/acp-20-539-2020, 2020.

Chang, Z., Shen, G., Jiang, K., Huang, W., Zhao, J., Luo, Z., Men, Y., Xing, R., Zhao, N., Pan, B., Xing, B., and Tao, S.: Environmental implications of residual pyrogenic carbonaceous materials from incomplete biomass combustion: a review, Carbon Res., 3, 15, https://doi.org/10.1007/s44246-024-00103-6, 2024.

Chao, A., Al-Ghoul, H., McEachran, A. D., Balabin, I., Transue, T., Cathey, T., Grossman, J. N., Singh, R. R., Ulrich, E. M., and Williams, A. J.: In silico MS/MS spectra for identifying unknowns: a critical examination using CFM-ID algorithms and ENTACT mixture samples, Anal. Bioanal. Chem., 412, 1303–1315, 2020.

Che, H., Segal-Rozenhaimer, M., Zhang, L., Dang, C., Zuidema, P., Dobracki, A., Sedlacek, A. J., Coe, H., Wu, H., Taylor, J., Zhang, X., Redemann, J., and Haywood, J.: Cloud processing and weeklong ageing affect biomass burning aerosol properties over the south-eastern Atlantic, Commun. Earth Environ., 3, 182, https://doi.org/10.1038/s43247-022-00517-3, 2022.

Chen, Y. and Bond, T. C.: Light absorption by organic carbon from wood combustion, Atmos. Chem. Phys., 10, 1773–1787, https://doi.org/10.5194/acp-10-1773-2010, 2010.

Choudhary, V., Roson, M. L., Guo, X., Gautam, T., Gupta, T., and Zhao, R.: Aqueous-phase photochemical oxidation of water-soluble brown carbon aerosols arising from solid biomass fuel burning, Environ. Sci.: Atmos., 3, 816–829, https://doi.org/10.1039/d2ea00151a, 2023.

D'Andrilli, J., Cooper, W. T., Foreman, C. M., and Marshall, A. G.: An ultrahigh-resolution mass spectrometry index to estimate natural organic matter lability, Rapid Commun. Mass Spectrom., 29, 2385–2401, https://doi.org/10.1002/rcm.7400, 2015.

Divisekara, D. T. D. K.: UHPLC/FT-MS Non-Targeted Screening Approach for Biomass Burning Organic Aerosol and Liquid Smoke as Biomass Burning Organic Aerosol Surrogate, Michigan Technological University, 2023.

Divisekara, T., Schum, S., and Mazzoleni, L.: Ultrahigh performance LC/FT-MS non-targeted screening for biomass burning organic aerosol with MZmine2 and MFAssignR, Chemosphere, 338, 139403, https://doi.org/10.1016/j.chemosphere.2023.139403, 2023.

Evans, R. L., Bryant, D. J., Voliotis, A., Hu, D., Wu, H., Syafira, S. A., Oghama, O. E., McFiggans, G., Hamilton, J. F., and Rickard, A. R.: A Semi-Quantitative Approach to Nontarget Compositional Analysis of Complex Samples, Anal. Chem., 96, 18349–18358, https://doi.org/10.1021/acs.analchem.4c00819, 2024.

Evans, R. L., Bryant, D. J., Voliotis, A., Hu, D., Wu, H., Syafira, S. A., Oghama, O. E., McFiggans, G., Hamilton, J. F., and Rickard, A. R.: The importance of burning conditions on the composition of domestic biomass-burning organic aerosol and the impact of atmospheric ageing, Atmos. Chem. Phys., 25, 4367–4389, https://doi.org/10.5194/acp-25-4367-2025, 2025.

Fleming, L. T., Lin, P., Laskin, A., Laskin, J., Weltman, R., Edwards, R. D., Arora, N. K., Yadav, A., Meinardi, S., Blake, D. R., Pillarisetti, A., Smith, K. R., and Nizkorodov, S. A.: Molecular composition of particulate matter emissions from dung and brushwood burning household cookstoves in Haryana, India, Atmos. Chem. Phys., 18, 2461–2480, https://doi.org/10.5194/acp-18-2461-2018, 2018.

Fleming, L. T., Lin, P., Roberts, J. M., Selimovic, V., Yokelson, R., Laskin, J., Laskin, A., and Nizkorodov, S. A.: Molecular composition and photochemical lifetimes of brown carbon chromophores in biomass burning organic aerosol, Atmos. Chem. Phys., 20, 1105–1129, https://doi.org/10.5194/acp-20-1105-2020, 2020.

Gadaleta, D., Vuković, K., Toma, C., Lavado, G. J., Karmaus, A. L., Mansouri, K., Kleinstreuer, N. C., Benfenati, E., and

Roncaglioni, A.: SAR and QSAR modeling of a large collection of LD50 rat acute oral toxicity data, J. Cheminformatics., 11, 58, https://doi.org/10.1186/s13321-019-0383-2, 2019.

Gao, P., Deng, R., Jia, S., Li, Y., Wang, X., and Xing, Q.: Effects of combustion temperature on the optical properties of brown carbon from biomass burning, J. Environ. Sci., 137, 302–309, https://doi.org/10.1016/j.jes.2022.12.026, 2024.

Go, B. R., Li, Y. J., Huang, D. D., and Chan, C. K.: Aqueous-Phase Photoreactions of Mixed Aromatic Carbonyl Photosensitizers Yield More Oxygenated, Oxidized, and less Light-Absorbing Secondary Organic Aerosol (SOA) than Single Systems, Environ. Sci. Technol., 58, 7924–7936, https://doi.org/10.1021/acs.est.3c10199, 2024.

Graham, B., Mayol-Bracero, O. L., Guyon, P., Roberts, G. C., Decesari, S., Facchini, M. C., Artaxo, P., Maenhaut, W., Köll, P., and Andreae, M. O.: Water-soluble organic compounds in biomass burning aerosols over Amazonia 1. Characterization by NMR and GC-MS, J. Geophys. Res.-Atmos., 107, LBA 14-11–LBA 14-16, https://doi.org/10.1029/2001JD000336, 2002.

Hartner, E., Gawlitta, N., Gröger, T., Orasche, J., Czech, H., Geldenhuys, G.-L., Jakobi, G., Tiitta, P., Yli-Pirilä, P., Kortelainen, M., Sippula, O., Forbes, P., and Zimmermann, R.: Chemical Fingerprinting of Biomass Burning Organic Aerosols from Sugar Cane Combustion: Complementary Findings from Field and Laboratory Studies, ACS Earth Space Chem., 8, 533–546, https://doi.org/10.1021/acsearthspacechem.3c00301, 2024.

Hems, R. F. and Abbatt, J. P. D.: Aqueous Phase Photo-oxidation of Brown Carbon Nitrophenols: Reaction Kinetics, Mechanism, and Evolution of Light Absorption, ACS Earth Space Chem., 2, 225–234, https://doi.org/10.1021/acsearthspacechem.7b00123, 2018.

Hems, R. F., Schnitzler, E. G., Bastawrous, M., Soong, R., Simpson, A. J., and Abbatt, J. P. D.: Aqueous Photoreactions of Wood Smoke Brown Carbon, ACS Earth Space Chem., 4, 1149–1160, https://doi.org/10.1021/acsearthspacechem.0c00117, 2020.

Herraiz, T. and Galisteo, J.: Hydroxyl radical reactions and the radical scavenging activity of β-carboline alkaloids, Food Chem., 172, 640–649, https://doi.org/10.1016/j.foodchem.2014.09.091, 2015.

Herrmann, H., Schaefer, T., Tilgner, A., Styler, S. A., Weller, C., Teich, M., and Otto, T.: Tropospheric aqueous-phase chemistry: kinetics, mechanisms, and its coupling to a changing gas phase, Chem. Rev., 115, 4259–4334, https://doi.org/10.1021/cr500447k, 2015.

Heuckeroth, S., Damiani, T., Smirnov, A., Mokshyna, O., Brungs, C., Korf, A., Smith, J. D., Stincone, P., Dreolin, N., Nothias, L.-F., Hyötyläinen, T., Orešič, M., Karst, U., Dorrestein, P. C., Petras, D., Du, X., van der Hooft, J. J. J., Schmid, R., and Pluskal, T.: Reproducible mass spectrometry data processing and compound annotation in MZmine 3, Nat. Protoc., 19, 2597–2641, https://doi.org/10.1038/s41596-024-00996-y, 2024.

Hohrenk, L. L., Itzel, F., Baetz, N., Tuerk, J., Vosough, M., and Schmidt, T. C.: Comparison of Software Tools for Liquid Chromatography-High-Resolution Mass Spectrometry Data Processing in Nontarget Screening of Environmental Samples, Anal. Chem., 92, 1898–1907, https://doi.org/10.1021/acs.analchem.9b04095, 2020.

Hu, D. and Yu, J. Z.: Secondary organic aerosol tracers and malic acid in Hong Kong: seasonal trends and origins, Environ. Chem., 10, 381–394, 2013.

Huang, R.-J., Yang, L., Shen, J., Yuan, W., Gong, Y., Ni, H., Duan, J., Yan, J., Huang, H., You, Q., and Li, Y. J.: Chromophoric Fingerprinting of Brown Carbon from Residential Biomass Burning, Environ. Sci. Technol. Lett., 9, 102–111, https://doi.org/10.1021/acs.estlett.1c00837, 2022.

Hulleman, T., Turkina, V., O'Brien, J. W., Chojnacka, A., Thomas, K. V., and Samanipour, S.: Critical Assessment of the Chemical Space Covered by LC–HRMS Non-Targeted Analysis, Environ. Sci. Technol., 57, 14101–14112, https://doi.org/10.1021/acs.est.3c03606, 2023.

Jiang, K., Xing, R., Luo, Z., Huang, W., Yi, F., Men, Y., Zhao, N., Chang, Z., Zhao, J., Pan, B., and Shen, G.: Pollutant emissions from biomass burning: A review on emission characteristics, environmental impacts, and research perspectives, Particuology, 85, 296–309, https://doi.org/10.1016/j.partic.2023.07.012, 2024.

Jiang, W., Misovich, M. V., Hettiyadura, A. P. S., Laskin, A., McFall, A. S., Anastasio, C., and Zhang, Q.: Photosensitized Reactions of a Phenolic Carbonyl from Wood Combustion in the Aqueous Phase – Chemical Evolution and Light Absorption Properties of AqSOA, Environ. Sci. Technol., 55, 5199–5211, https://doi.org/10.1021/acs.est.0c07581, 2021.

Jones, M. W., Kelley, D. I., Burton, C. A., Di Giuseppe, F., Barbosa, M. L. F., Brambleby, E., Hartley, A. J., Lombardi, A., Mataveli, G., McNorton, J. R., Spuler, F. R., Wessel, J. B., Abatzoglou, J. T., Anderson, L. O., Andela, N., Archibald, S., Armenteras, D., Burke, E., Carmenta, R., Chuvieco, E., Clarke, H., Doerr, S. H., Fernandes, P. M., Giglio, L., Hamilton, D. S., Hantson, S., Harris, S., Jain, P., Kolden, C. A., Kurvits, T., Lampe, S., Meier, S., New, S., Parrington, M., Perron, M. M. G., Qu, Y., Ribeiro, N. S., Saharjo, B. H., San-Miguel-Ayanz, J., Shuman, J. K., Tanpipat, V., van der Werf, G. R., Veraverbeke, S., and Xanthopoulos, G.: State of Wildfires 2023–2024, Earth Syst. Sci. Data, 16, 3601–3685, https://doi.org/10.5194/essd-16-3601-2024, 2024.

Kahn, R. A., Andrews, E., Brock, C. A., Chin, M., Feingold, G., Gettelman, A., Levy, R. C., Murphy, D. M., Nenes, A., Pierce, J. R., Popp, T., Redemann, J., Sayer, A. M., da Silva, A. M., Sogacheva, L., and Stier, P.: Reducing Aerosol Forcing Uncertainty by Combining Models With Satellite and Within-The-Atmosphere Observations: A Three-Way Street, Rev. Geophys., 61, e2022RG000796, https://doi.org/10.1029/2022RG000796, 2023.

Kawamoto, H.: Lignin pyrolysis reactions, J. Wood Sci., 63, 117–132, 2017.

Khan, F., Kwapiszewska, K., Zhang, Y., Chen, Y., Lambe, A. T., Kołodziejczyk, A., Jalal, N., Rudzinski, K., Martínez-Romero, A., Fry, R. C., Surratt, J. D., and Szmigielski, R.: Toxicological Responses of α-Pinene-Derived Secondary Organic Aerosol and Its Molecular Tracers in Human Lung Cell Lines, Chem. Res. Toxicol, 34, 817–832, https://doi.org/10.1021/acs.chemrestox.0c00409, 2021.

Koch, B. P. and Dittmar, T.: From mass to structure: an aromaticity index for high-resolution mass data of natural organic matter, Rapid Commun. Mass Spectrom., 20, 926–932, https://doi.org/10.1002/rcm.2386, 2006.

Kroll, J. H., Donahue, N. M., Jimenez, J. L., Kessler, S. H., Canagaratna, M. R., Wilson, K. R., Altieri, K. E., Mazzoleni, L. R.,

Wozniak, A. S., and Bluhm, H.: Carbon oxidation state as a metric for describing the chemistry of atmospheric organic aerosol, Nat. Chem., 3, 133–139, 2011.

Kruve, A.: Semi-quantitative non-target analysis of water with liquid chromatography/high-resolution mass spectrometry: How far are we?, Rapid Commun. Mass Spectrom., 33, 54–63, 2019.

Kuang, X. M., Gonzalez, D. H., Scott, J. A., Vu, K., Hasson, A., Charbouillot, T., Hawkins, L., and Paulson, S. E.: Cloud Water Chemistry Associated with Urban Aerosols: Rapid Hydroxyl Radical Formation, Soluble Metals, Fe(II), Fe(III), and Quinones, ACS Earth Space Chem., 4, 67–76, https://doi.org/10.1021/acsearthspacechem.9b00243, 2020.

Kumar, B., Schumacher, J., and Shaw, R. A.: Cloud microphysical effects of turbulent mixing and entrainment, Theor. Comput. Fluid Dyn., 27, 361–376, https://doi.org/10.1007/s00162-012-0272-z, 2013.

Lai, Z., Tsugawa, H., Wohlgemuth, G., Mehta, S., Mueller, M., Zheng, Y., Ogiwara, A., Meissen, J., Showalter, M., Takeuchi, K., Kind, T., Beal, P., Arita, M., and Fiehn, O.: Identifying metabolites by integrating metabolome databases with mass spectrometry cheminformatics, Nat. Methods, 15, 53–56, https://doi.org/10.1038/nmeth.4512, 2018.

Laskin, A., West, C. P., and Hettiyadura, A. P. S.: Molecular insights into the composition, sources, and aging of atmospheric brown carbon, Chem. Soc. Rev., 54, 1583–1612, https://doi.org/10.1039/D3CS00609C, 2025.

Laszakovits, J. R. and MacKay, A. A.: Data-based chemical class regions for Van Krevelen diagrams, J. Am. Soc. Mass Spectrom., 33, 198–202, 2021.

Lei, R., Sha, Y., Meng, H., Huang, Y., Ye, J., Huang, D. D., Zhang, Y., Wu, Y., Li, Y., and Ge, X.: Aqueous phase photolysis of 4-nitrocatechol: Reaction kinetics, evolutions of chemical composition, light absorption and oxidation potential, Atmos. Environ., 343, 120981, https://doi.org/10.1016/j.atmosenv.2024.120981, 2025.

Li, L., Han, Y., Li, J., Lin, Y., Zhang, X., Wang, Q., and Cao, J.: Effects of photochemical aging on the molecular composition of organic aerosols derived from agricultural biomass burning in whole combustion process, Sci. Total Environ., 946, 174152, https://doi.org/10.1016/j.scitotenv.2024.174152, 2024.

Li, S., Zhang, H., Wang, Z., and Chen, Y.: Advances in the Research on Brown Carbon Aerosols: Its Concentrations, Radiative Forcing, and Effects on Climate, Aerosol Air Qual. Res., 23, 220336, https://doi.org/10.4209/aaqr.220336, 2023.

Li, W., Ge, P., Chen, M., Tang, J., Cao, M., Cui, Y., Hu, K., and Nie, D.: Tracers from Biomass Burning Emissions and Identification of Biomass Burning, Atmosphere, 12, 1401, https://doi.org/10.3390/atmos12111401, 2021a.

Li, Y., Kind, T., Folz, J., Vaniya, A., Mehta, S. S., and Fiehn, O.: Spectral entropy outperforms MS/MS dot product similarity for small-molecule compound identification, Nat. Methods, 18, 1524–1531, 2021b.

Lin, P., Aiona, P. K., Li, Y., Shiraiwa, M., Laskin, J., Nizkorodov, S. A., and Laskin, A.: Molecular Characterization of Brown Carbon in Biomass Burning Aerosol Particles, Environ. Sci. Technol., 50, 11815–11824, https://doi.org/10.1021/acs.est.6b03024, 2016.

Lin, P., Fleming, L. T., Nizkorodov, S. A., Laskin, J., and Laskin, A.: Comprehensive Molecular Characterization of Atmospheric Brown Carbon by High Resolution Mass Spectrometry with Electrospray and Atmospheric Pressure Photoionization, Anal. Chem., 90, 12493–12502, https://doi.org/10.1021/acs.analchem.8b02177, 2018.

Liu, D., He, C., Schwarz, J. P., and Wang, X.: Lifecycle of light-absorbing carbonaceous aerosols in the atmosphere, Npj Clim. Atmos. Sci., 3, 40, https://doi.org/10.1038/s41612-020-00145-8, 2020.

Liu, Y., Chen, J., Shi, Y., Zheng, W., Shan, T., and Wang, G.: Global Emissions Inventory from Open Biomass Burning (GEIOBB): utilizing Fengyun-3D global fire spot monitoring data, Earth Syst. Sci. Data, 16, 3495–3515, https://doi.org/10.5194/essd-16-3495-2024, 2024.

Ma, Y.-J., Xu, Y., Yang, T., Xiao, H.-W., and Xiao, H.-Y.: Measurement report: Characteristics of nitrogen-containing organics in $PM_{2.5}$ in Ürümqi, northwestern China – differential impacts of combustion of fresh and aged biomass materials, Atmos. Chem. Phys., 24, 4331–4346, https://doi.org/10.5194/acp-24-4331-2024, 2024.

Majewska, M., Khan, F., Pieta, I. S., Wróblewska, A., Szmigielski, R., and Pieta, P.: Toxicity of selected airborne nitrophenols on eukaryotic cell membrane models, Chemosphere, 266, 128996, https://doi.org/10.1016/j.chemosphere.2020.128996, 2021.

Mallmann, L. P., O. Rios, A., and Rodrigues, E.: MS-FINDER and SIRIUS for phenolic compound identification from high-resolution mass spectrometry data, Int. Food Res., 163, 112315, https://doi.org/10.1016/j.foodres.2022.112315, 2023.

Malm, L., Palm, E., Souihi, A., Plassmann, M., Liigand, J., and Kruve, A.: Guide to Semi-Quantitative Non-Targeted Screening Using LC/ESI/HRMS, Molecules, 26, 3524, https://doi.org/10.3390/molecules26123524, 2021.

Mansouri, K., Grulke, C. M., Judson, R. S., and Williams, A. J.: OPERA models for predicting physicochemical properties and environmental fate endpoints, J. Cheminformatics., 10, 10, https://doi.org/10.1186/s13321-018-0263-1, 2018.

Mansouri, K., Karmaus, A. L., Fitzpatrick, J., Patlewicz, G., Pradeep, P., Alberga, D., Alepee, N., Allen, T. E., Allen, D., and Alves, V. M.: CATMoS: collaborative acute toxicity modeling suite, Environ. Health Perspect., 129, 047013, https://doi.org/10.1289/EHP8495, 2021.

Matsui, H., Hamilton, D. S., and Mahowald, N. M.: Black carbon radiative effects highly sensitive to emitted particle size when resolving mixing-state diversity, Nat. Commun., 9, 3446, https://doi.org/10.1038/s41467-018-05635-1, 2018.

Merel, S.: Critical assessment of the Kendrick mass defect analysis as an innovative approach to process high resolution mass spectrometry data for environmental applications, Chemosphere, 313, 137443, https://doi.org/10.1016/j.chemosphere.2022.137443, 2023.

Moise, T., Flores, J. M., and Rudich, Y.: Optical Properties of Secondary Organic Aerosols and Their Changes by Chemical Processes, Chem. Rev., 115, 4400–4439, https://doi.org/10.1021/cr5005259, 2015.

MoNa [data set]: Downloads, https://mona.fiehnlab.ucdavis.edu/downloads (last access date: 8 August 2024), 2024.

Moschos, V., Christensen, C., Mouton, M., Fiddler, M. N., Isolabella, T., Mazzei, F., Massabò, D., Turpin, B. J., Bililign, S., and Surratt, J. D.: Quantifying the Light-Absorption Properties and Molecular Composition of Brown Carbon Aerosol from Sub-

Saharan African Biomass Combustion, Environ. Sci. Technol., 58, 4268–4280, https://doi.org/10.1021/acs.est.3c09378, 2024.

MS-DIAL: MS-DIAL metabolomics MSP spectral kit containing EI-MS, MS/MS, and CCS values, https://systemsomicslab.github.io/compms/msdial/main.html#MSP, last access: 8 August 2024.

Narukawa, M., Kawamura, K., Takeuchi, N., and Nakajima, T.: Distribution of dicarboxylic acids and carbon isotopic compositions in aerosols from 1997 Indonesian forest fires, Geophys. Res. Lett., 26, 3101–3104, 1999.

Ng, B.: Non-Target Analysis Using High-Resolution Mass Spectrometry to Characterize and Remediate Urban Waters, https://digitalcommons.fiu.edu/etd/4856/, 2021.

Nihill, K. J., Coggon, M. M., Lim, C. Y., Koss, A. R., Yuan, B., Krechmer, J. E., Sekimoto, K., Jimenez, J. L., de Gouw, J., Cappa, C. D., Heald, C. L., Warneke, C., and Kroll, J. H.: Evolution of organic carbon in the laboratory oxidation of biomass-burning emissions, Atmos. Chem. Phys., 23, 7887–7899, https://doi.org/10.5194/acp-23-7887-2023, 2023.

Nizkorodov, S. A., Laskin, J., and Laskin, A.: Molecular chemistry of organic aerosols through the application of high resolution mass spectrometry, Phys. Chem. Chem. Phys., 13, 3612–3629, https://doi.org/10.1039/c0cp02032j, 2011.

Noblet, C., Lestremau, F., Collet, S., Chatellier, C., Beaumont, J., Besombes, J. L., and Albinet, A.: Aerosolomics based approach to discover source molecular markers: A case study for discriminating residential wood heating vs garden green waste burning emission sources, Chemosphere, 352, 141242, https://doi.org/10.1016/j.chemosphere.2024.141242, 2024.

Oros, D. R. and Simoneit, B. R. T.: Identification and emission factors of molecular tracers in organic aerosols from biomass burning Part 2. Deciduous trees, Appl. Geochem., 16, 1545–1565, https://doi.org/10.1016/S0883-2927(01)00022-1, 2001.

Oros, D. R., Abas, M. R. b., Omar, N. Y. M. J., Rahman, N. A., and Simoneit, B. R. T.: Identification and emission factors of molecular tracers in organic aerosols from biomass burning: Part 3. Grasses, Appl. Geochem., 21, 919–940, https://doi.org/10.1016/j.apgeochem.2006.01.008, 2006.

Pan, X., Ichoku, C., Chin, M., Bian, H., Darmenov, A., Colarco, P., Ellison, L., Kucsera, T., da Silva, A., Wang, J., Oda, T., and Cui, G.: Six global biomass burning emission datasets: intercomparison and application in one global aerosol model, Atmos. Chem. Phys., 20, 969–994, https://doi.org/10.5194/acp-20-969-2020, 2020.

Pang, Z., Lu, Y., Zhou, G., Hui, F., Xu, L., Viau, C., Spigelman, Aliya F., MacDonald, Patrick E., Wishart, David S., Li, S., and Xia, J.: MetaboAnalyst 6.0: towards a unified platform for metabolomics data processing, analysis and interpretation, Nucleic Acids Res., 52, W398–W406, https://doi.org/10.1093/nar/gkae253, 2024.

Paulson, S. E., Gallimore, P. J., Kuang, X. M., Chen, J. R., Kalberer, M., and Gonzalez, D. H.: A light-driven burst of hydroxyl radicals dominates oxidation chemistry in newly activated cloud droplets, Sci. Adv., 5, eaav7689, https://doi.org/10.1126/sciadv.aav7689, 2019.

Pflieger, M. and Kroflič, A.: Acute toxicity of emerging atmospheric pollutants from wood lignin due to biomass burning, J. Hazard. Mater., 338, 132–139, https://doi.org/10.1016/j.jhazmat.2017.05.023, 2017.

Pieke, E. N., Granby, K., Trier, X., and Smedsgaard, J.: A framework to estimate concentrations of potentially unknown substances by semi-quantification in liquid chromatography electrospray ionization mass spectrometry, Anal. Chim. Acta, 975, 30–41, https://doi.org/10.1016/j.aca.2017.03.054, 2017.

Pokhrel, R. P., Gordon, J., Fiddler, M. N., and Bililign, S.: Determination of Emission Factors of Pollutants From Biomass Burning of African Fuels in Laboratory Measurements, J. Geophys. Res., 126, e2021JD034731, https://doi.org/10.1029/2021jd034731, 2021.

Priestley, M., Kong, X., Pei, X., Pathak, R. K., Davidsson, K., Pettersson, J. B. C., and Hallquist, M.: Volatility Measurements of Oxygenated Volatile Organics from Fresh and Aged Residential Wood Burning Emissions, ACS Earth Space Chem., 8, 159–173, https://doi.org/10.1021/acsearthspacechem.3c00066, 2024.

Rivera-Pérez, A. and Garrido Frenich, A.: Comparison of data processing strategies using commercial vs. open-source software in GC-Orbitrap-HRMS untargeted metabolomics analysis for food authentication: thyme geographical differentiation and marker identification as a case study, Anal. Bioanal. Chem., 416, 4039–4055, https://doi.org/10.1007/s00216-024-05347-0, 2024.

Russo, F. F., Nowatzky, Y., Jaeger, C., Parr, M. K., Benner, P., Muth, T., and Lisec, J.: Machine learning methods for compound annotation in non-targeted mass spectrometry – A brief overview of fingerprinting, in silico fragmentation and de novo methods, Rapid Commun. Mass Spectrom., 38, e9876, https://doi.org/10.1002/rcm.9876, 2024.

Růžičková, J., Raclavská, H., Šafář, M., Kucbel, M., Raclavský, K., Grobelak, A., Švédová, B., and Juchelková, D.: The occurrence of pesticides and their residues in char produced by the combustion of wood pellets in domestic boilers, Fuel, 293, 120452, https://doi.org/10.1016/j.fuel.2021.120452, 2021.

Saleh, R.: From Measurements to Models: Toward Accurate Representation of Brown Carbon in Climate Calculations, Curr. Pollut. Rep., 6, 90–104, https://doi.org/10.1007/s40726-020-00139-3, 2020.

Sanches-Neto, F. O., Dias-Silva, J. R., Keng Queiroz Junior, L. H., and Carvalho-Silva, V. H.: "pySiRC": Machine Learning Combined with Molecular Fingerprints to Predict the Reaction Rate Constant of the Radical-Based Oxidation Processes of Aqueous Organic Contaminants, Environ. Sci. Technol., 55, 12437–12448, https://doi.org/10.1021/acs.est.1c04326, 2021.

Sander, R.: Compilation of Henry's law constants (version 4.0) for water as solvent, Atmos. Chem. Phys., 15, 4399–4981, https://doi.org/10.5194/acp-15-4399-2015, 2015.

Sarang, K., Otto, T., Rudzinski, K., Schaefer, T., Grgić, I., Nestorowicz, K., Herrmann, H., and Szmigielski, R.: Reaction Kinetics of Green Leaf Volatiles with Sulfate, Hydroxyl, and Nitrate Radicals in Tropospheric Aqueous Phase, Environ. Sci. Technol., 55, 13666–13676, https://doi.org/10.1021/acs.est.1c03276, 2021.

Schmid, R., Heuckeroth, S., Korf, A., Smirnov, A., Myers, O., Dyrlund, T. S., Bushuiev, R., Murray, K. J., Hoffmann, N., Lu, M., Sarvepalli, A., Zhang, Z., Fleischauer, M., Dührkop, K., Wesner, M., Hoogstra, S. J., Rudt, E., Mokshyna, O., Brungs, C., Ponomarov, K., Mutabdžija, L., Damiani, T., Pudney, C. J., Earll, M., Helmer, P. O., Fallon, T. R., Schulze, T., Rivas-Ubach, A., Bilbao, A., Richter, H., Nothias, L.-F., Wang, M., Orešič, M., Weng, J.-K., Böcker, S., Jeibmann, A.,

Hayen, H., Karst, U., Dorrestein, P. C., Petras, D., Du, X., and Pluskal, T.: Integrative analysis of multimodal mass spectrometry data in MZmine 3, Nature Biotechnology, 41, 447–449, https://doi.org/10.1038/s41587-023-01690-2, 2023.

Schymanski, E. L., Jeon, J., Gulde, R., Fenner, K., Ruff, M., Singer, H. P., and Hollender, J.: Identifying Small Molecules via High Resolution Mass Spectrometry: Communicating Confidence, Environ. Sci. Technol., 48, 2097–2098, https://doi.org/10.1021/es5002105, 2014.

Sekimoto, K., Koss, A. R., Gilman, J. B., Selimovic, V., Coggon, M. M., Zarzana, K. J., Yuan, B., Lerner, B. M., Brown, S. S., Warneke, C., Yokelson, R. J., Roberts, J. M., and de Gouw, J.: High- and low-temperature pyrolysis profiles describe volatile organic compound emissions from western US wildfire fuels, Atmos. Chem. Phys., 18, 9263–9281, https://doi.org/10.5194/acp-18-9263-2018, 2018.

Sengupta, D., Samburova, V., Bhattarai, C., Watts, A. C., Moosmüller, H., and Khlystov, A. Y.: Polar semivolatile organic compounds in biomass-burning emissions and their chemical transformations during aging in an oxidation flow reactor, Atmos. Chem. Phys., 20, 8227–8250, https://doi.org/10.5194/acp-20-8227-2020, 2020.

Seo, I., Lee, K., Bae, M. S., Park, M., Maskey, S., Seo, A., Borlaza, L. J. S., Cosep, E. M. R., and Park, K.: Comparison of physical and chemical characteristics and oxidative potential of fine particles emitted from rice straw and pine stem burning, Environ. Pollut., 267, 115599, https://doi.org/10.1016/j.envpol.2020.115599, 2020.

Shahid, I., Kistler, M., Shahid, M. Z., and Puxbaum, H.: Aerosol Chemical Characterization and Contribution of Biomass Burning to Particulate Matter at a Residential Site in Islamabad, Pakistan, Aerosol Air Qual. Res., 19, 148–162, https://doi.org/10.4209/aaqr.2017.12.0573, 2019.

Shen, M., Ho, K. F., Dai, W., Liu, S., Zhang, T., Wang, Q., Meng, J., Chow, J. C., Watson, J. G., Cao, J., and Li, J.: Distribution and stable carbon isotopic composition of dicarboxylic acids, ketocarboxylic acids and α-dicarbonyls in fresh and aged biomass burning aerosols, Atmos. Chem. Phys., 22, 7489–7504, https://doi.org/10.5194/acp-22-7489-2022, 2022.

Siemens, K., Morales, A., He, Q., Li, C., Hettiyadura, A. P. S., Rudich, Y., and Laskin, A.: Molecular Analysis of Secondary Brown Carbon Produced from the Photooxidation of Naphthalene, Environ. Sci. Technol., 56, 3340–3353, https://doi.org/10.1021/acs.est.1c03135, 2022.

Simoneit, B. R. T.: Biomass burning – a review of organic tracers for smoke from incomplete combustion, Appl. Geochem., 17, 129–162, https://doi.org/10.1016/S0883-2927(01)00061-0, 2002.

Sinha, A., George, I., Holder, A., Preston, W., Hays, M., and Grieshop, A. P.: Development of Volatility Distributions for Organic Matter in Biomass Burning Emissions, Environ. Sci. Atmos., 3, 11–23, https://doi.org/10.1039/d2ea00080f, 2023.

Smith, D. M., Cui, T., Fiddler, M. N., Pokhrel, R. P., Surratt, J. D., and Bililign, S.: Laboratory studies of fresh and aged biomass burning aerosol emitted from east African biomass fuels – Part 2: Chemical properties and characterization, Atmos. Chem. Phys., 20, 10169–10191, https://doi.org/10.5194/acp-20-10169-2020, 2020.

Smith, J. S., Laskin, A., and Laskin, J.: Molecular characterization of biomass burning aerosols using high-resolution mass spectrometry, Anal. Chem., 81, 1512–1521, 2009.

Song, J., Li, M., Jiang, B., Wei, S., Fan, X., and Peng, P.: Molecular Characterization of Water-Soluble Humic like Substances in Smoke Particles Emitted from Combustion of Biomass Materials and Coal Using Ultrahigh-Resolution Electrospray Ionization Fourier Transform Ion Cyclotron Resonance Mass Spectrometry, Environ. Sci. Technol., 52, 2575–2585, https://doi.org/10.1021/acs.est.7b06126, 2018.

Stubenrauch, J. and Garske, B.: Forest protection in the EU's renewable energy directive and nature conservation legislation in light of the climate and biodiversity crisis – Identifying legal shortcomings and solutions, For. Policy Econ., 153, 102996, https://doi.org/10.1016/j.forpol.2023.102996, 2023.

Su, H., Cheng, Y., and Pöschl, U.: New Multiphase Chemical Processes Influencing Atmospheric Aerosols, Air Quality, and Climate in the Anthropocene, Acc. Chem. Res., 53, 2034–2043, https://doi.org/10.1021/acs.accounts.0c00246, 2020.

Su, Q.-Z., Vera, P., and Nerín, C.: Combination of Structure Databases, In Silico Fragmentation, and MS/MS Libraries for Untargeted Screening of Non-Volatile Migrants from Recycled High-Density Polyethylene Milk Bottles, Anal. Chem., 95, 8780–8788, https://doi.org/10.1021/acs.analchem.2c05389, 2023.

Sun, M., Glenn, C. K., El Hajj, O., Kumar, K. V., Anosike, A., Penland, R., Callaham, M. A., Jr., Loudermilk, E. L., O'Brien, J. J., Saleh, R., and Smith, G. D.: Aqueous Photolysis of Water-Soluble Brown Carbon from Simulated Prescribed and Wildfire Biomass Burning, ACS ES&T Air, 1, 989–999, https://doi.org/10.1021/acsestair.4c00016, 2024.

Tang, J., Li, J., Su, T., Han, Y., Mo, Y., Jiang, H., Cui, M., Jiang, B., Chen, Y., Tang, J., Song, J., Peng, P., and Zhang, G.: Molecular compositions and optical properties of dissolved brown carbon in biomass burning, coal combustion, and vehicle emission aerosols illuminated by excitation–emission matrix spectroscopy and Fourier transform ion cyclotron resonance mass spectrometry analysis, Atmos. Chem. Phys., 20, 2513–2532, https://doi.org/10.5194/acp-20-2513-2020, 2020.

Tomlin, A. S.: Air Quality and Climate Impacts of Biomass Use as an Energy Source: A Review, Energy & Fuels, 35, 14213–14240, https://doi.org/10.1021/acs.energyfuels.1c01523, 2021.

Trubetskaya, A.: Reactivity Effects of Inorganic Content in Biomass Gasification: A Review, Energies, 15, 3137, https://doi.org/10.3390/en15093137, 2022.

Tsigaridis, K. and Kanakidou, M.: The Present and Future of Secondary Organic Aerosol Direct Forcing on Climate, Curr. Clim. Change Rep., 4, 84–98, https://doi.org/10.1007/s40641-018-0092-3, 2018.

Tsugawa, H., Kanazawa, M., Ogiwara, A., and Arita, M.: MRMPROBS suite for metabolomics using large-scale MRM assays, Bioinformatics, 30, 2379–2380, https://doi.org/10.1093/bioinformatics/btu203, 2014.

Tsugawa, H., Cajka, T., Kind, T., Ma, Y., Higgins, B., Ikeda, K., Kanazawa, M., VanderGheynst, J., Fiehn, O., and Arita, M.: MS-DIAL: data-independent MS/MS deconvolution for comprehensive metabolome analysis, Nat Methods, 12, 523–526, https://doi.org/10.1038/nmeth.3393, 2015.

Tsugawa, H., Kind, T., Nakabayashi, R., Yukihira, D., Tanaka, W., Cajka, T., Saito, K., Fiehn, O., and Arita, M.: Hydrogen Rearrangement Rules: Computational MS/MS Fragmentation and Structure Elucidation Using MS-FINDER Software, Anal. Chem., 88, 7946–7958, https://doi.org/10.1021/acs.analchem.6b00770, 2016.

Vaniya, A., Samra, S. N., Palazoglu, M., Tsugawa, H., and Fiehn, O.: Using MS-FINDER for identifying 19 natural products in the CASMI 2016 contest, Phytochem. Lett., 21, 306–312, https://doi.org/10.1016/j.phytol.2016.12.008, 2017.

Vosough, M., Schmidt, T. C., and Renner, G.: Non-target screening in water analysis: recent trends of data evaluation, quality assurance, and their future perspectives, Anal. Bioanal. Chem., 416, 2125–2136, https://doi.org/10.1007/s00216-024-05153-8, 2024.

Wan, X., Kawamura, K., Ram, K., Kang, S., Loewen, M., Gao, S., Wu, G., Fu, P., Zhang, Y., Bhattarai, H., and Cong, Z.: Aromatic acids as biomass-burning tracers in atmospheric aerosols and ice cores: A review, Environ. Pollut. , 247, 216–228, https://doi.org/10.1016/j.envpol.2019.01.028, 2019.

Wang, F., Liigand, J., Tian, S., Arndt, D., Greiner, R., and Wishart, D. S.: CFM-ID 4.0: More Accurate ESI-MS/MS Spectral Prediction and Compound Identification, Anal. Chem., 93, 11692–11700, https://doi.org/10.1021/acs.analchem.1c01465, 2021.

Wartmann, Y., Boxler, M. I., Kraemer, T., and Steuer, A. E.: Impact of three different peak picking software tools on the quality of untargeted metabolomics data, J. Pharm. Biomed. Anal., 248, 116302, https://doi.org/10.1016/j.jpba.2024.116302, 2024.

Wei, M., Xu, C., Xu, X., Zhu, C., Li, J., and Lv, G.: Characteristics of atmospheric bacterial and fungal communities in PM2.5 following biomass burning disturbance in a rural area of North China Plain, Sci. Total Environ., 651, 2727–2739, https://doi.org/10.1016/j.scitotenv.2018.09.399, 2019.

Witkowski, B., Jain, P., and Gierczak, T.: Aqueous chemical bleaching of 4-nitrophenol brown carbon by hydroxyl radicals; products, mechanism, and light absorption, Atmos. Chem. Phys., 22, 5651–5663, https://doi.org/10.5194/acp-22-5651-2022, 2022.

Wong, J. P. S., Tsagkaraki, M., Tsiodra, I., Mihalopoulos, N., Violaki, K., Kanakidou, M., Sciare, J., Nenes, A., and Weber, R. J.: Effects of Atmospheric Processing on the Oxidative Potential of Biomass Burning Organic Aerosols, Environ. Sci. Technol., 53, 6747–6756, https://doi.org/10.1021/acs.est.9b01034, 2019.

Yadav, I. C. and Devi, N. L.: Biomass Burning, Regional Air Quality, and Climate Change, in: Encyclopedia of Environmental Health (Second Edition), edited by: Nriagu, J., Elsevier, Oxford, 386–391, https://doi.org/10.1016/B978-0-12-409548-9.11022-X, 2019.

Yadav, S., Kapoor, T. S., Vernekar, P., and Phuleria, H. C.: Examining the Chemical and Optical Properties of Biomass-burning Aerosols and their Impact on Oxidative Potential, Aerosol Air Qual. Res., 23, 230102, https://doi.org/10.4209/aaqr.230102, 2023.

Yang, Y., Li, C., Yang, L., Zheng, M., and Liu, G.: Application of non-target screening by high-resolution mass spectrometry to identification and control of new contaminants: Implications for sustainable industrial development, Sustainable Horizons, 5, 100049, https://doi.org/10.1016/j.horiz.2023.100049, 2023.

Yee, L. D., Kautzman, K. E., Loza, C. L., Schilling, K. A., Coggon, M. M., Chhabra, P. S., Chan, M. N., Chan, A. W. H., Hersey, S. P., Crounse, J. D., Wennberg, P. O., Flagan, R. C., and Seinfeld, J. H.: Secondary organic aerosol formation from biomass burning intermediates: phenol and methoxyphenols, Atmos. Chem. Phys., 13, 8019–8043, https://doi.org/10.5194/acp-13-8019-2013, 2013.

Young, T. M., Black, G. P., Wong, L., Bloszies, C. S., Fiehn, O., He, G., Denison, M. S., Vogel, C. F. A., and Durbin-Johnson, B.: Identifying Toxicologically Significant Compounds in Urban Wildfire Ash Using In Vitro Bioassays and High-Resolution Mass Spectrometry, Environ. Sci. Technol., 55, 3657–3667, https://doi.org/10.1021/acs.est.0c06712, 2021.

Zhang, L., Li, J., Li, Y., Liu, X., Luo, Z., Shen, G., and Tao, S.: Comparison of water-soluble and water-insoluble organic compositions attributing to different light absorption efficiency between residential coal and biomass burning emissions, Atmos. Chem. Phys., 24, 6323–6337, https://doi.org/10.5194/acp-24-6323-2024, 2024.

Zhao, R., Lee, A. K. Y., Huang, L., Li, X., Yang, F., and Abbatt, J. P. D.: Photochemical processing of aqueous atmospheric brown carbon, Atmos. Chem. Phys., 15, 6087–6100, https://doi.org/10.5194/acp-15-6087-2015, 2015.

Zherebker, A., Babcock, O., Pereira, D. L., D'Aronco, S., Filippi, D., Soldà, L., Michoud, V., Gratien, A., Cirtog, M., and Cantrell, C.: Decreasing the Uncertainty in the Comparison of Molecular Fingerprints of Organic Aerosols with H/D Exchange Mass Spectrometry, Environ. Sci. Technol., 58, 20468–20479, 2024.

Zhou, Y., West, C. P., Hettiyadura, A. P. S., Niu, X., Wen, H., Cui, J., Shi, T., Pu, W., Wang, X., and Laskin, A.: Measurement report: Molecular composition, optical properties, and radiative effects of water-soluble organic carbon in snowpack samples from northern Xinjiang, China, Atmos. Chem. Phys., 21, 8531–8555, https://doi.org/10.5194/acp-21-8531-2021, 2021.